Innovative Infrastructure Solutions (2025) 10:396
https://doi.org/10.1007/s41062-025-02206-4

PRACTICE-ORIENTED PAPER

An alternative sustainable desert-sand concrete incorporating industrial waste fillers: physicomechanical and microstructural insights

Mohamed Merniz[1] · Madani Bederina[1] · Abdelaziz Meddah[2] · Lysandros Pantelidis[3] · Ammar Noui[4]

Received: 1 March 2025 / Accepted: 23 July 2025

Abstract

The growing demand for sustainable construction materials has led to increased interest in utilizing industrial waste in concrete production. In particular, the replacement of conventional fillers with recycled materials presents both environmental and technical advantages. This study investigates the partial replacement of limestone filler (LF), with two powdered materials, waste glass powder (WGP) and waste expanded perlite (WEP), in desert sand concrete (DSC). The Design of Experiments technique was employed to assess the influence of these substitutions on the fresh and hardened properties of DSC, including workability, compressive strength, thermal conductivity, water absorption, and microstructure. Results showed that combining LF and WGP improved workability by up to 15.27%, while WEP tended to reduce it. Thermal conductivity was significantly reduced by WEP, achieving up to 15.29% reduction at full replacement. Compressive strength increased by up to 56% at 90 days with WGP, while ternary blends (LF–WGP–WEP) improved strength by 11.9%–24.85% compared to the control mix. Full replacement of LF with WGP also reduced water absorption by approximately 35.52%. SEM and EDX analyses revealed that WGP enhanced the microstructure and promoted C–S–H formation, contributing to reduced porosity and improved performance. These findings highlight the sustainable potential of reusing industrial waste in DSC to achieve both environmental and technical benefits. The approach supports circular economy principles and presents a promising solution for eco-efficient construction in arid regions.

Keywords Desert-sand concrete · Sustainable concrete · Glass powder · Expanded perlite · Limestone · Waste

Abbreviations

LF	Limestone filler
WGP	Glass powder
WEP	Expanded perlite powder
DSC	Desert-sand concrete
DS	Desert sand
RS	River sand
RG	Recycled glass
DOE	Design of experiments
SEM	Scanning electron microscopy
EDS	Energy dispersive spectroscopy
TC	Thermal conductivity

✉ Abdelaziz Meddah
abdelaziz.meddah@univ-msila.dz

1 SRML, Civil Engineering Department, University of Amar Télidji, Laghouat, Algeria

2 LDGM, Civil Engineering Department, University of M'sila, 28000 Msila, Algeria

3 Department of Civil Engineering and Geomatics, Cyprus University of Technology, Limassol, Cyprus

4 Civil Engineering Department, University Mohamed El Bachir El Ibrahimi, Bordj Bou Arreridj, Algeria

Introduction

In the last decades, the construction industry has faced several significant challenges, such as insufficient supply of essential raw materials, high energy consumption, considerable CO_2 emissions, and accumulation of waste in open areas, all negatively impacting the environment. As a result, researchers have increasingly focused on recovering local materials and integrating waste in construction materials, including vegetal, mineral, and metallic waste [1, 2]. This

Published online: 13 August 2025

practice not only helps mitigate the environmental impact of waste but also offers a potential solution for its disposal [3, 4]. Recent studies further indicate that the depletion raw material and mismanaging waste can be addressed by valorizing untapped local resources and recycling discarded materials [1, 5, 6].

In ordinary concrete, natural sand constitutes approximately 25–28% of the total aggregate volume. Despite its relatively small proportion, it plays an important role in determining the properties of the concrete [7, 8]. This role is even more significant in sand concrete, where the total volume of aggregates is entirely sand. In many regions, rivers serve as the main source of sand (river sand, RS) for concrete production. However, the increasing scarcity of such materials due to overuse and ecological harm is causing significant environmental and economic challenges, making the exploration of alternative resources crucial [9, 10].

In this context, Desert Sand (DS) emerges as a promising alternative. Abundant in arid regions like the Sahara, DS has gained increasing attention for its potential use as fine aggregates in concrete and mortar [11, 12]. For instance, Bederina et al. [13] demonstrated that using DS and RS in specific proportions, along with LF, can produce sand concrete that meets essential workability and strength requirements. With the depletion of RS, using DS in sustainable construction practices offers an attractive solution to address the growing demand for sand in the construction industry [9, 14].

Huynh et al. [9] reported that the total replacement of RS with DS reduces workability, mechanical strength, and ultrasonic pulse velocity while increasing drying shrinkage, porosity, water absorption, and chloride permeability. Nevertheless, mixtures containing 50% or 100% DS combined with 35% ground granulated blast furnace slag showed significant performance improvements, surpassing the minimum requirements for most construction applications.

Similarly, Kaufmann [15] investigated using DS in combination with calcium sulfoaluminate cement as an eco-friendly alternative to traditional Portland cement. The high gypsum content in this cement promoted ettringite formation, retaining mixing water and addressing the high water demand of DS. This approach produces a denser microstructure and improved mechanical performance. Additionally, Wang et al. [16] investigated the freeze–thaw resistance of 3D-printed composites with DS, finding that a sand-to-cement (S/C) ratio of 1.7 offered optimal mechanical performance and freeze–thaw resistance. Dong et al. [17] explored the partial replacement (0 to 40%) of RS with DS in lightweight pozzolan aggregate concrete, and their results indicated that substitution rates of 20–30% improved freeze–thaw resistance.

In parallel with the research on alternative aggregates, the recycling of industrial waste materials presents another promising way to improve the sustainability of concrete. Glass waste, which is often disposed of in landfills, has gained attention as an alternative to both natural aggregates and cement. Sustainable development demands efficient waste management, reduced landfill use, and increased recycling and reuse in civil engineering [18]. Reusing glass waste as a substitute for natural aggregates or Portland cement has been widely studied to address the approximately 200 million tons of glass landfilled annually. However, global recycling rates remain low despite ongoing efforts. Given the rising consumption of glass products, recycling offers a practical solution. Over the last two decades, numerous studies have confirmed the feasibility of incorporating recycled glass (RG) in concrete, either as a partial or full replacement for aggregates [19–21] or as a partial replacement for cement [21–23].

Previous studies highlight uncertainties regarding the impact of RG, in both powder or coarse form, on the workability of concrete mixtures. The mechanical properties of concrete are primarily influenced by the fineness of the incorporated RG and the curing age of concrete [24, 25]. Most studies report that RG decreases thermal conductivity, improves thermal properties, and reduces sorptivity. For example, Sikora [26] and Maglad [27] showed that fine RG aggregates can successfully replace natural fine sand without adversely affecting the mechanical performance of concrete.

Ammari et al. [28] found that partially replacing cement with WGP enhances the flexural and compressive strength of sand concrete by up to 9% and 18%, respectively, with an optimal WGP addition of 10%, whereas thermal conductivity and shrinkage were reduced by 12.74% and 20%, respectively. Similarly, Shayan [29] showed that WGP could replace up to 30% of cement in 40 MPa concrete, achieving 55 MPa at 404 days while improving resistance to chloride penetration and lowering greenhouse gas emissions.

In addition to glass, expanded perlite (an amorphous volcanic rock) offers potential as a sustainable additive. Its lightweight porous structure provides excellent thermal and acoustic insulation, but its production generates waste [29, 30]. Studies, such as those conducted by Long et al. [31] and Kotwica et al. [32, 33], demonstrated that WEP enhances hydration, reduces embodied CO_2 emissions, and improves thermal properties in cementitious materials, despite slight reductions in compressive strength. Pichor et al. [34] reported that substituting sand with WEP reduces density and improves the thermal conductivity of autoclave concrete while maintaining reasonable compressive strength up to a 10% replacement.

When aggregate size decreases to ≤ 6 mm, as in sand concrete, the cement dosage significantly increases (>400 kg/m^3) due to the smaller, more numerous voids that require

Table 1 Physical and chemical properties of raw materials

Raw materials	Physical properties				Chemical composition (%)				
	Absolute density	Apparent density	Fineness modulus (cm^2/g)	Sand equivalent (%)	CaO	SiO_2	Al_2O_3	Fe_2O_3	SO_3
Cement	3.1	–	3700–5200	–	70.41	14.329	6.759	3.902	3.059
DS	2.6	1.577	–	88.23	2.15	92.473	4.040	0.569	0.000
WEP	0.6	0.34	2150–3100	–	1.52	77.33	13.369	1.326	0.000
WGP	2.57	1.62	2200–2800	–	15.45	81.90	1.46	0.48	0.30
LF	2.7	1.61	2500	–	87.45	3.731	6.053	1.565	0.044

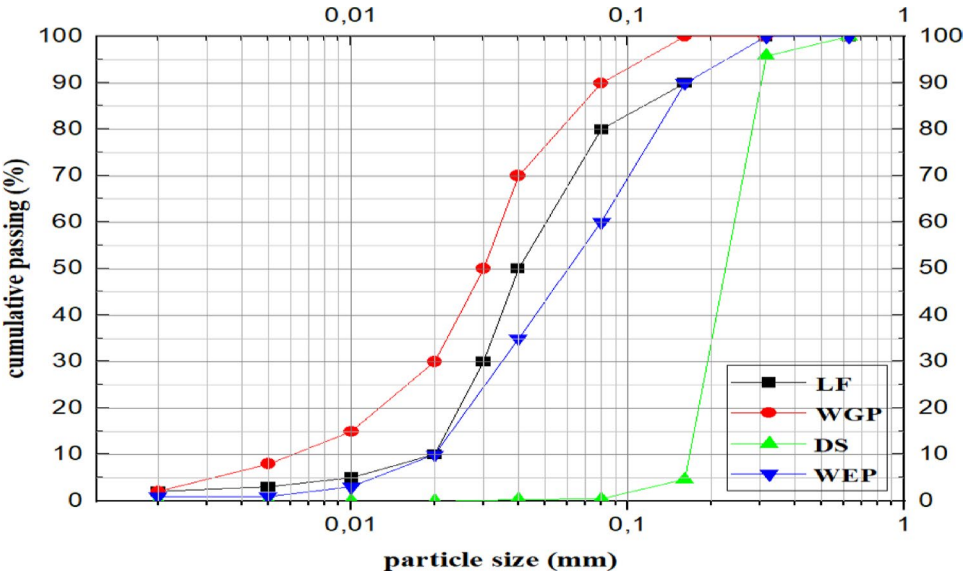

Fig. 1 Particle size distribution curves for raw materials

filling. This creates technical and economic challenges as the balance between cement and fine materials becomes inconsistent. In sand concrete, voids are initially filled with fillers, and rigidity is achieved using additional cement, typically matching traditional concrete dosages. High quantities of fillers (70–220 kg/m^3 or more) are required, and their properties (e.g., geological origin and shape) strongly affect the performance of this material [35]. LF waste (fraction smaller than 80 µm produced during aggregate crushing), is commonly used. Research on replacing or combining LF with other materials remains limited, although using such fillers aligns with recycling efforts for industrial waste [36–40].

This study aims to partially and fully replace LF with two powdered industrial wastes, including WGP and WEP, in DSC. Using DOE, the research evaluates the fresh and hardened properties of sand concrete, including workability, mechanical strength, thermal conductivity, and water absorption. Microstructural analyses are also conducted to explore the effects of their combination. The novelty of this research lies in its innovative strategy, which is to substitute conventional fillers (LF) with recycled industrial waste materials (WGP and WEP), thereby aligning with circular economy principles. This innovative approach promotes the sustainable use of resources, reduces the environmental impact of industrial waste, and improves the mechanical and functional performance of DSC. By integrating waste valorization in construction practices, this study addresses critical sustainability challenges while advancing the development of eco-friendly, high-performance materials.

Materials and methods

Materials

- The cement used for producing the studied DSC is of type CEM II/B- 42.5N, complied with the European standard [41], distributed by LAFARGE cement company (Algeria). This cement is used in high-performance concrete for civil engineering structures. The physical and chemical properties of the cement are shown in Table 1.
- A clean DS collected from the Bousaâda region in Algeria, part of arid zones, was used in the study. Its granulometric distribution curve shows that this sand has a maximum grain diameter of approximately 0.63 mm, with fines content (<0.08 mm) of less than 5%, as illustrated in Fig. 1. X-ray diffraction analysis shows that the sand is primarily siliceous, as shown in Fig. 2. The

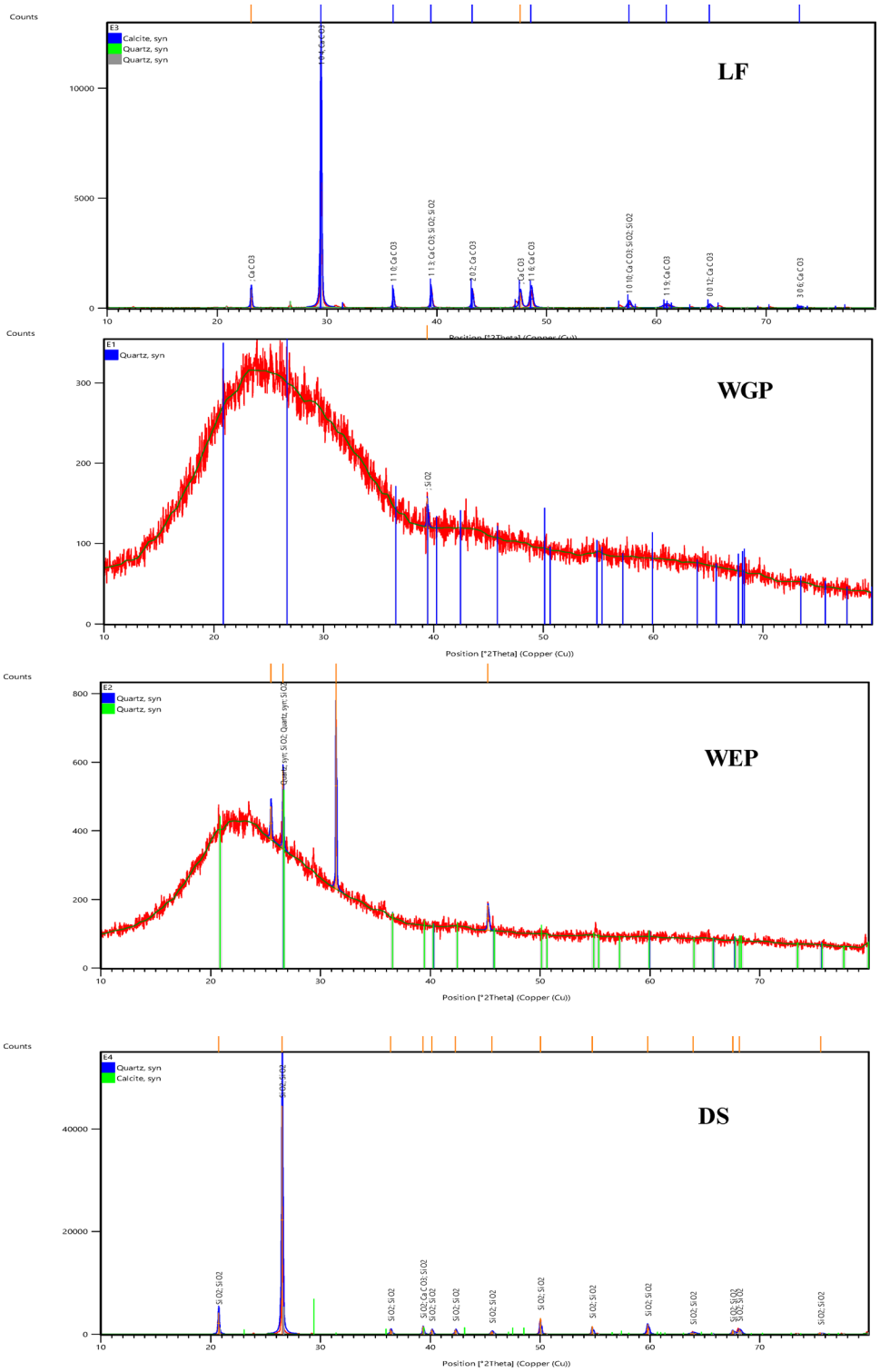

Fig. 2 The X-ray diffraction (XRD) patterns for different quantities of materials used

main physical and chemical characteristics of the sand are provided in Table 1.

- Three types of inert fillers LF, WGP, and WEP were introduced into the study, contributing to sustainability and circular economy principles as highlighted in previous research [42–44]. LF used was produced by the National Aggregates Company (ENG) of Algeria. WGP was obtained by grinding waste glass using a Los Angeles apparatus with metal balls. WEP was provided by the "Taouab" factory in Algeria. During the processing and filtering of WEP, a significant amount of powder is generated, making it a valuable resource for construction,

particularly in desert sand concrete (DSC) applications. All fillers used in the experimental program were in powdered form (particle size smaller than 0.08 mm), with their granulometric distributions shown in Fig. 1, while their meniragical compositions are illustrated in Fig. 2. The main physical and chemical characteristics of these fillers are presented in Table 1.

- A high water-reducing superplasticizer, "MEDAFLOW 30" was used. This liquid solution complies with EN 934-2 [45] and can be easily diluted in the mixing water.

Methods

Mixture design

This study builds on the same mix design proportions used in previous studies [13, 40] while incorporating industrial wastes, aiming to enhance the performance of DSC for sustainable and innovative construction practices. The base mix proportions and the design of the concrete mixes for the 21 experimental tests, developed using the DOE method, are presented in Table 2. This table includes the quantities of all mix components, including the varying proportions of fillers (LF, WGP, and WEP) used in each mixture.

The DOE method was employed to systematically evaluate the influence of different waste materials on the properties of DSC. This approach facilitates the optimization of ingredients while minimizing experimental efforts and ensuring a comprehensive assessment of the key factors such as workability, strength, thermal conductivity, and water absorption of DSC. By focusing on the most significant variables, DOE ensures more reliable, data-driven results [42, 46, 47]. DOE is widely applicable across disciplines and industries, especially when investigating the relationship between a variable of interest, Y (e.g., concrete properties), and input variables X_i (e.g., proportions of the component materials). Indeed, it is relevant to use "experimental design" methods when we are interested in a function of the type [48]:

$$Y = f(X_i) \tag{1}$$

In an experiment, the "response" is the measured quantity of interest, while the variables influencing it are called "factors". DOE enables obtaining maximum information with minimal experimentation by adhering to strict mathematical principles. Two key concepts underlie DOE: the experimental space and the mathematical modeling of the quantities studied.

The study's factors for the mixture design are the proportions of the mixture's constituents, which are interdependent because their sum must always equal 100%. Denoting X_i as the content of constituent i, this relationship is expressed as:

$$\sum_{i=1}^{i=n} X_i = 100\% \tag{2}$$

Table 2 Detailed mixture compositions derived from the designated mixing plan

Mixture	Additives in concrete per unit 1			Additives in concrete per (kg/m^3)			Sand (kg/m^3)	Cement (kg/m^3)	Water (l/m3)	Sp (%)
	LF	WGP	WEP	LF	WGP	WEP				
DSC 1	1	0	0	200	0	0	1305	350	245	2
DSC 2	0.8	0.2	0	160	38	0				
DSC 3	0.6	0.4	0	120	75	0				
DSC 4	0.4	0.6	0	80	113	0				
DSC 5	0.2	0.8	0	40	150	0				
DSC 6	0	1	0	0	188	0				
DSC 7	0.8	0	0.2	160	0	9				
DSC 8	0.6	0	0.4	120	0	18				
DSC 9	0.4	0	0.6	80	0	27				
DSC 10	0.2	0	0.8	40	0	36				
DSC 11	0	0	1	0	0	45				
DSC 12	0	0.8	0.2	0	150	9				
DSC 13	0	0.6	0.4	0	113	18				
DSC 14	0	0.4	0.6	0	75	27				
DSC 15	0	0.2	0.8	0	38	36				
DSC 16	0.6	0.2	0.2	120	38	9				
DSC 17	0.2	0.2	0.6	40	38	27				
DSC 18	0.2	0.6	0.2	40	113	9				
DSC 19	0.4	0.4	0.2	80	75	9				
DSC 20	0.4	0.2	0.4	80	38	18				
DSC 21	0.2	0.4	0.4	40	75	18				

The primary objective of this study is to partially or entirely replace LF with WGP and WEP, two types of waste materials (WGP, and WEP), as schematized in Fig. 3. Various binary and ternary combinations were examined to compressively assess the effects of these fillers on the properties of DSC both in the fresh and hardened states. To achieve this, the mixture design considered three factors (LF, WGP, and WEP) expressed as volume proportions, with the constraint [49]:

$$\mathrm{WGP} + \mathrm{WEP} + \mathrm{LF} = 1 \tag{3}$$

For three factors (q), five levels of proportion (m) were selected to enhance the clarity of the study and its results. The number of experiments was calculated using the "combinations with repetition" formula:

$$C_{q+m-1}^{m} = \frac{(q+m-1)!}{(m)!\,(q-1)!} \tag{4}$$

Using $q = 3$ and $m = 5$, the calculation yielded:

$$C_{3+5-1}^{5} = \frac{7!}{5!.2!} = \frac{5040}{240} = 21$$

These 21 experiments were designed and analyzed using the JMP 18 statistical software developed for advanced data analysis, visualization, and design of experiments (DOE).

A second-degree polynomial model was developed to describe the influence of varying proportions of LF, WGP, and WEP on the selected properties of DSC. The model is expressed as:

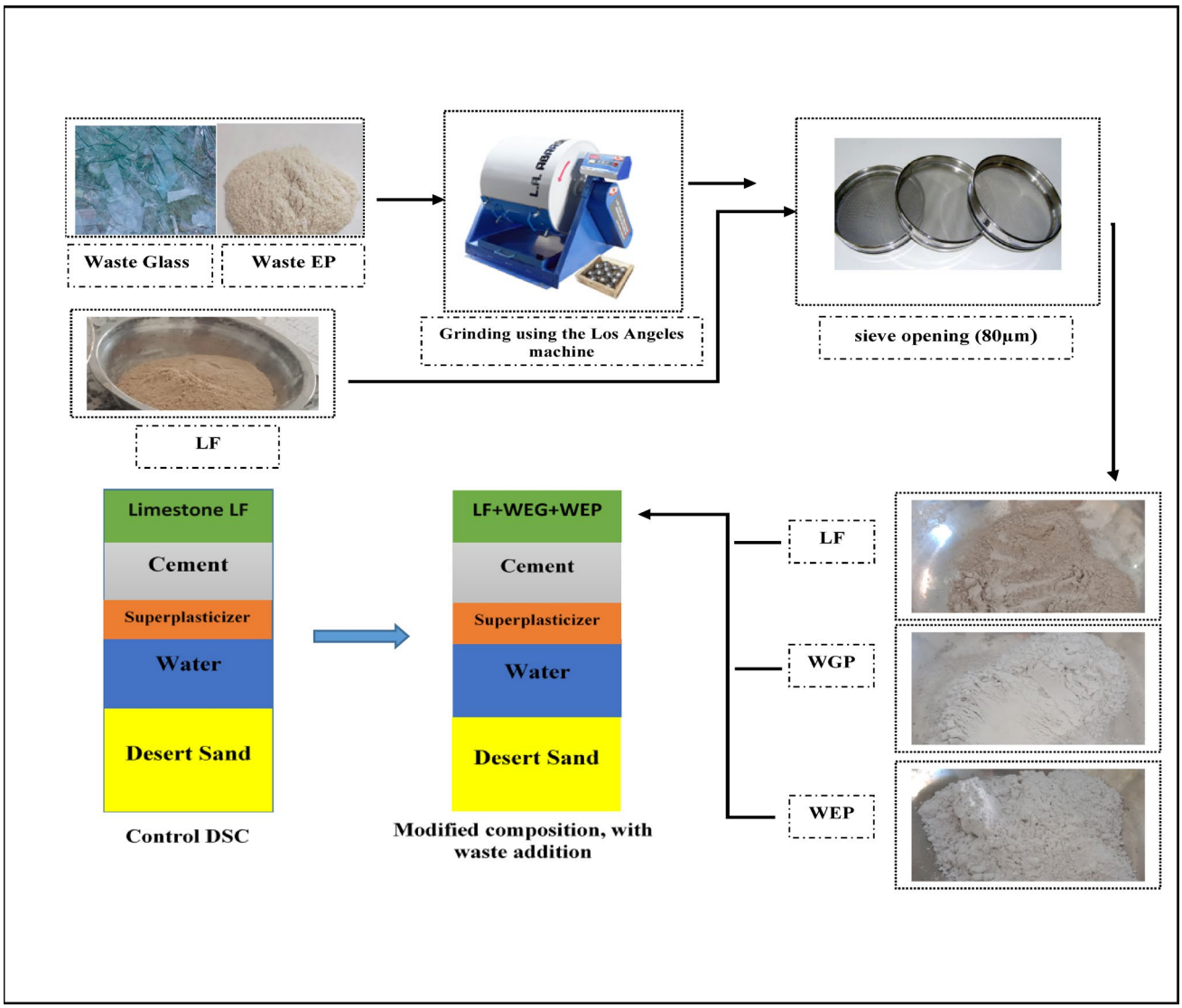

Fig. 3 Simplified schematic illustrating the approach used to incorporate filler waste into the concrete mix

$$Y = b_1 \cdot LF + b_2 \cdot WGP + b_3 \cdot WEP + b_4 \cdot (LF \cdot WGP) + b_5 \cdot (LF \cdot WEP) + b_6 \cdot (WGP \cdot WEP) \quad (5)$$

Here, the coefficients b_i represent the influence of each variable or interaction on the response (Y). These coefficients were determined using the standard least-squares fit method, and analysis of variance (ANOVA) was conducted to evaluate the significance of each term. Residuals were used to compute the variance of the coefficients, serving as the basis for testing their significance [49, 50].

Table 2 provides the detailed proportions of the mixtures in $\mathrm{kg/m^3}$. LF was replaced with WGP and WEP in proportions of 20%, 40%, 60%, 80%, and 100%. Binary mixtures of WGP and WEP were also considered in these proportions. Additionally, ternary mixtures involving LF, WGP, and WEP were prepared with proportions of 20%, 40%, and 60%.

An equilateral triangle was generated using JMP 18 software to represent the three-component mixtures. The vertices correspond to the pure components, while binary mixtures are represented along the sides (e.g., the left side of Fig. 4 shows mixtures of LF and WGP).

Using the same software, the responses obtained were represented by ternary diagrams that link the three components (LF, WGP, and WEP) to each studied property.

Mixture proportions and sample preparation

Concrete mixing was performed using an AUTOMIX mixer (Fig. 5). DS, cement, and fillers were first combined and mixed for one minute. Half of the water, premixed with the

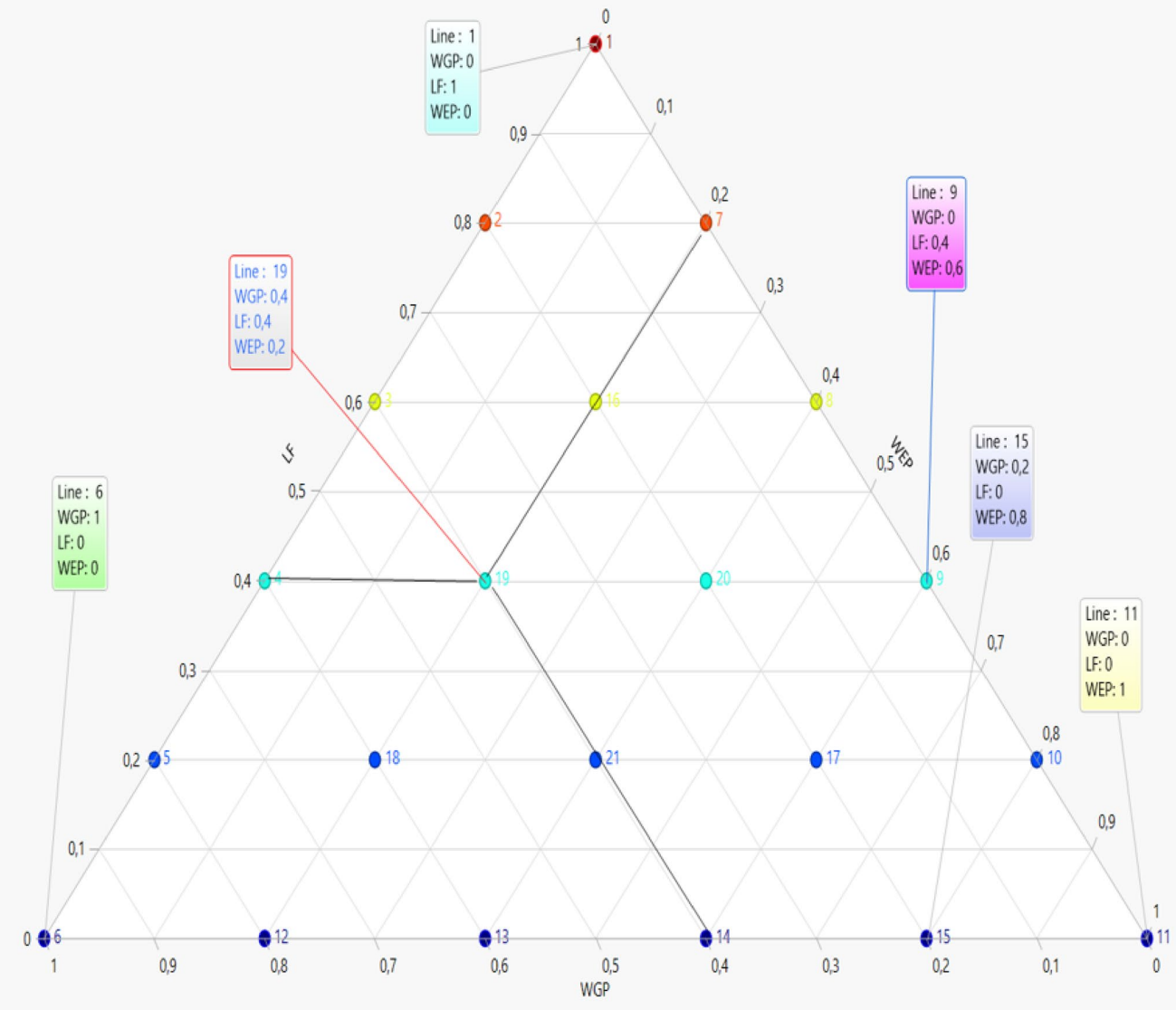

Fig. 4 Ternary diagram illustrating the 21 combinations of components evaluated in the study

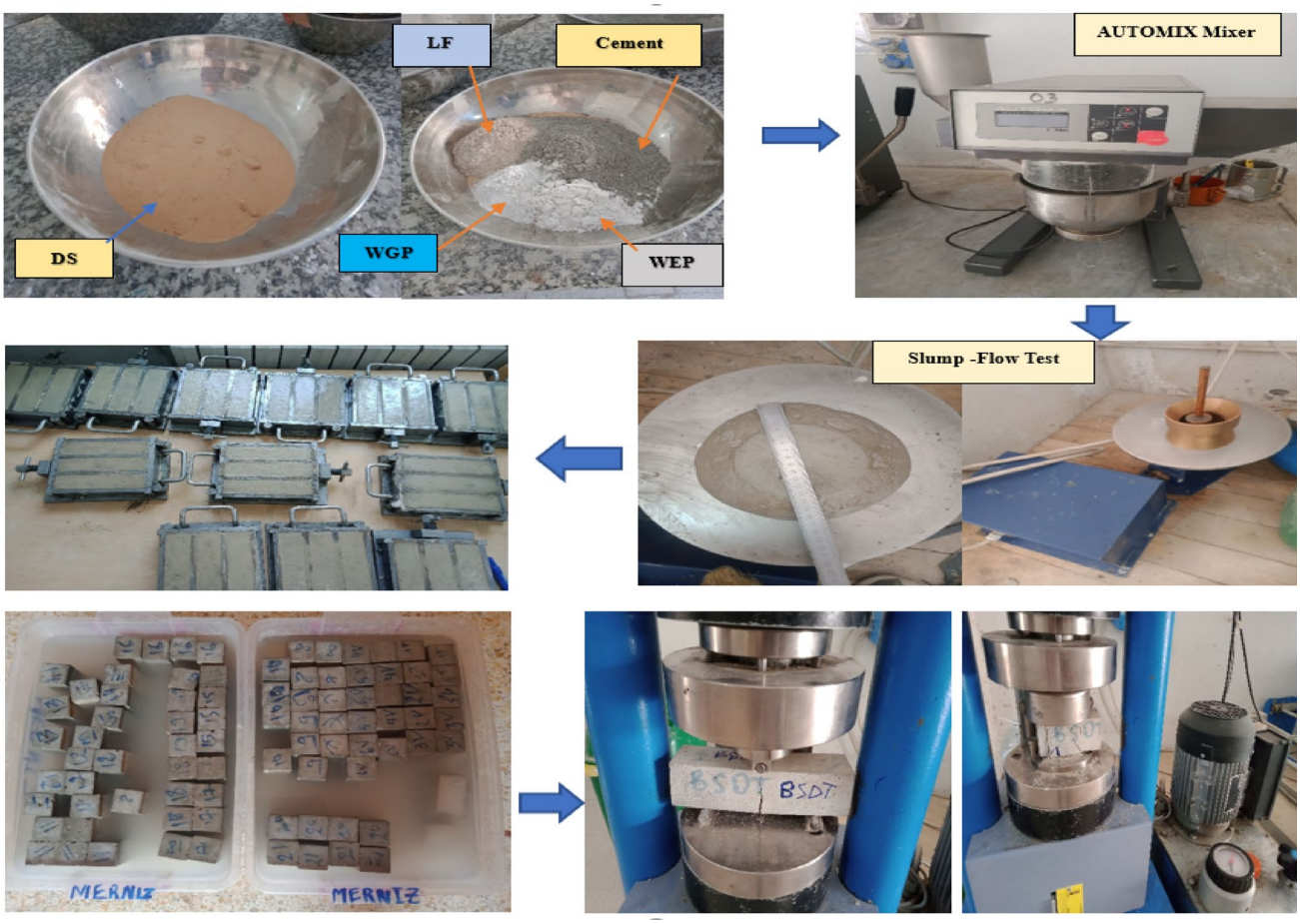

Fig. 5 Key steps involved in the sample preparation process

admixture, was then added and mixed for 30 s. The remaining water was subsequently added, and mixing continued for an additional two minutes to ensure thorough homogenization. Fresh concrete tests, including the shaking table spreading test, were then conducted. The concrete was poured into pre-oiled prismatic molds (40 × 40 × 160) mm and compacted on a vibrating table for 10 s to remove air bubbles and ensure optimal compactness.

Nine specimens were prepared for each mixture, including one designated for thermal conductivity testing using a "Hot Disk" apparatus after being cut to 40 mm × 40 mm × 20 mm. All specimens were cured in tap water at 20 ± 2 °C for 7 and 90 days.

Tests

The slump-flow test was performed in accordance to ASTM C1437 [51]. Water absorption by immersion was measured at 28 days following ASTM C642 [52]. Flexural strength tests were performed on 40 × 40 × 160 mm prisms at 7 and 90 days, in accordance with NF EN 12390-5 [53]. Compression tests were performed on 40 × 40 × 40 mm cubes as per NF EN 12390-4 [54].

Experimental results and discussions

Statistical models

A comprehensive statistical analysis was conducted to understand better the influence of the three key factors, LF, WGP, and WEP, on the properties of sand concrete. The goal was to develop predictive models that link these factors to critical material properties, including slump, compressive strength, thermal conductivity, and water absorption.

The analysis was conducted using a robust modeling approach known for its ability to generate visual representations such as iso-response curves with ternary diagrams (Fig. 4). These diagrams provide a clear understanding of how each factor, along with their interactions, influences the performance of the DSC mixtures.

Table 3 presents the regression coefficients, p-values, and correlation coefficients (R^2) for the predictive models

Table 3 Estimated model parameters for the investigated responses

Response	Slump test (%)		CS_{7j}		CS_{90j}		Thermal Conductivity		Water Abs. by immersion (%)	
Correlation coefficient (R^2)	0.86		0.83		0.88		0.70		0.92	
	Coeff	*p*-value	Coeff	*p*-value	Coeff	*p*-value	Coeff	*p*-value	Coeff	*p*-value
LF	74.166	<0.0001*	18.17	<0.0001*	26.89	<0.0001*	1.6678	<0.0001*	7.56	<0.0001*
WGP	60.952	<0.0001*	17.607	<0.0001*	38.98	<0.0001*	1.5711	<0.0001*	4.73	<0.0001*
WEP	32..976	<0.0001*	12.137	<0.0001*	23.86	<0.0001*	1.4693	<0.0001*	6.59	<0.0001*
LF.WGP	24.851	0.2953	7.174	0.1229	18.81	0.0234*	0.1474	0.4768	−5.36	0.0006*
LF.WEP	-30.208	0.2072	−10.730	0.0273*	−5.02	0.5198	−0.1516	0.4647	0.30	0.8072
WGP.WEP	-45.833	0.0639	0.8065	0.856	−7.36	0.3494	−0.3684	0.0883	−4.36	0.0028*

developed for each response. The exceptionally low *p*-values (<0.0001) for the primary factors LF, WGP, and WE demonstrate their significant influence on the studied properties. These results validate the inclusion of these factors in the models.

The final predictive models for the studied properties are represented by the following equations:

Slump:

$$S\,(\%) = 74.166LF + 60.952WGP + 32.976WEP + 24.851LF \cdot WGP - 30.208LF \cdot WEP - 45.833WGP \cdot WEP \quad (6)$$

7-days compressive strength (MPa):

$$CS_{7j} = 18.174LF + 17.607WGP + 12.137WEP + 7.17LF \cdot WGP - 10.730LF \cdot WEP + 0.80WGP \cdot WEP \quad (7)$$

90-days compressive strength (MPa):

$$CS_{90j} = 26.89LF + 38.98WGP + 23.87WEP + 18.81LF \cdot WGP - 5.02LF \cdot WEP - 7.36WGP \cdot WEP \quad (8)$$

Thermal conductivity $\left(\mathrm{W \cdot m^{-1}\,k^{-1}}\right)$:

$$T_c = 1.667LF + 1.571WGP + 1.469WEP + 0.147LF \cdot WGP - 0.151LF \cdot WEP - 0.368WGP \cdot WEP \quad (9)$$

Water absorption (%):

$$W_{ab} = 7.56LF + 4.73WGP + 6.59WEP - 5.33LF \cdot WGP + 0.30LF \cdot WEP - 4.36WGP * WEP \quad (10)$$

From the results of the statistical models:

- Slump (%):
  The slump of DSC increased with higher LF content, followed by WGP, reflecting improved workability. However, excessive WEP content reduces workability due to its lightweight and low density.
- Compressive strength:
  WGP had the strongest positive effect on compressive strength, especially at 90 days, enhancing the long-term mechanical performance of DSC. LF and WEP also contributed positively, though imbalances in their proportions slightly reduced strength in some instances.
- Thermal conductivity (W m^{-1} K^{-1}):
  LF made the most significant contribution to thermal conductivity, followed by WGP and WEP. Higher WEP levels slightly reduced conductivity, consistent with its insulating properties.
- Water absorption (%):
  Water absorption was most influenced by LF; WGP also had a positive impact. Their combination reduced water absorption, indicating a denser matrix and improved impermeability. However, higher WEP levels slightly increased absorption due to its effect on pore structure.
  These results underscore the potential of incorporating industrial wastes, such as WGP and WEP, into DSC for sustainable and innovative construction materials. The predictive models developed in this study enable the optimization of DSC mixtures, balancing workability, strength, thermal performance, and permeability to meet specific application needs (Fig. 6).

Slump flow test

Table 4 summarizes the results of the slump flow test conducted on the 21 DSC mixtures studied. The reference mix (100% LF), showed results consistent with a previous study [13], confirming its suitability as a benchmark. It was selected due to its superior performance in both fresh and hardened states, and served as baeline for evaluating the other mixtures.

Fig. 6 Equipment used for analyzing the thermal properties and microstructure of the samples **a** Hot Disk test **b** SEM test **c** XRF test **d** XRD test

The iso-response diagram in Fig. 7 illustrates the slump flow results across various proportions of LF, WGP, and WEP. The diagram employs color gradients to represent slump levels: lighter shades indicate lower slump values (approximately 30%), while darker shades represent higher slump values (up to 80%). This visual representation facilitates the identification of optimal component proportions for achieving desired workability levels, enabling precise adjustments to mix consistency.

From the iso-response curve (Fig. 7.a), the substitution of LF with WGP (DSC2, DSC3, and DSC4) resulted in notable workability improvements of 4.16%, 15.27%, and 11.11%, respectively, as also seen reported in Table 4. This enhancement can be attributed to the fine particle size of WGP, which fills microvoids more efficiently than LF, thus releasing trapped water and increasing concrete density. This observation aligns with earlier study [55] and correlates with the short-term compressive strength results at 7 days (refer to Table 4), which exceeded those of the reference concrete. It is important to note that the pozzolanic activity of glass powder typically develops fully in the long term [18, 56] further supporting these findings.

However, workability decreased to levels below the reference mix at higher proportions of WGP (80% and 100% substitution, i.e., DSC5 and DSC6), as seen in Fig. 7a and Table 4. This trend aligns with the findings of Rahma et al. [57], who observed reduced workability with increased WGP content. Despite its low water absorption, the fineness and high specific surface area of WGP create surface tension, effectively trapping water necessary for maintaining consistency. Nevertheless, the workability remained within acceptable limits, meeting the "plastic" classification as per ASTM C1437.

In the binary combinations of LF and WEP or WGP and WEP, as well as in ternary mixes incorporating all three components, an increase in WEP content led to a loss in workability, clearly observed in Fig. 7b and reflected in Table 6. This reduction can be explained by the high water absorption of WEP, which increases the water demand of the mix. These findings corroborate earlier study [58], where the porous microstructure and large specific surface area of perlite were identified as primary contributors to higher water requirements [59, 60].

Table 4 Results of characterization testing for the investigated responses

Mixture	Additives proportions in concrete			Compressive strength (MPa)		Slump test (%)	Hardened density of concrete (kg/m^3)	W. Abs. by immersion (%)	Th. conductivity W m^{-1} k^{-1}
	LF	WGP	WEP	7 days	90 days				
DSC 1	1	0	0	18.88	26.72	72	1835.9	7.02	1.713
DSC 2	0.8	0.2	0	19.24	32.35	75	1863.2	6.28	1.693
DSC 3	0.6	0.4	0	21	38.88	80	1902.3	5.33	1.67
DSC 4	0.4	0.6	0	19.17	37.05	83	1937.5	4.43	1.636
DSC 5	0.2	0.8	0	18.2	38.65	65	1957	4.39	1.679
DSC 6	0	1	0	17.37	41.89	60	1898.4	4.52	1.568
DSC 7	0.8	0	0.2	13.18	25.45	63	1785.1	7.87	1.526
DSC 8	0.6	0	0.4	12.72	23.7	60	1851.5	7.59	1.563
DSC 9	0.4	0	0.6	11.73	22.24	45	1835.9	6.80	1.522
DSC 10	0.2	0	0.8	13	22.51	35	1820.3	6.86	1.470
DSC 11	0	0	1	12.02	22.45	30	1742.1	6.95	1.451
DSC 12	0	0.8	0.2	18.76	33.34	45	1878.9	4.78	1.504
DSC 13	0	0.6	0.4	15.33	28.98	45	1894.5	4.53	1.374
DSC 14	0	0.4	0.6	14.26	27.24	40	1882.8	5.18	1.473
DSC 15	0	0.2	0.8	12.148	28.44	30	1847.6	5.07	1.385
DSC 16	0.6	0.2	0.2	17.46	29.9	50	1914	6.32	1.540
DSC 17	0.2	0.2	0.6	13.48	30.53	45	1847.6	5.28	1.575
DSC 18	0.2	0.6	0.2	15.72	33.36	52	1875	4.375	1.440
DSC 19	0.4	0.4	0.2	15.34	30.46	55	1875	5.20	1.522
DSC 20	0.4	0.2	0.4	16.52	31.48	40	1882.8	5.39	1.561
DSC 21	0.2	0.4	0.4	16.05	31.78	35	1875	4.79	1.565

Compressive strength

The iso-response diagram (Fig. 8) illustrates the 7-day compressive strength of sand concrete as a function of the proportions of LF, WEP, and WGP. The color gradients on the diagram indicate compressive strength levels, with numerical values corresponding to the experimental results for each mix. The color gradients in the diagram represent compressive strength levels, with lighter shades indicating lower strengths (around 12 MPa) and darker shades indicating higher strengths (up to 21 MPa). The diagram identifies optimal component proportions to achieve desired strength levels.

From the results, it is evident that supplementary cementitious materials (SCMs) influence compressive strength through three primary mechanisms: (i) the filling effect, (ii) the acceleration of ordinary Portland cement (OPC) hydration, and (iii) the pozzolanic reaction [61].

As shown in Table 4, mixes with higher slump flow values also exhibited higher 7-day compressive strength. This improvement is attributed to the combination of LF and WGP, which effectively fills voids and releases trapped water. The differences in fineness and morphology between LF and WGP likely contribute to this beneficial physical effect. Previous studies support these observations. For instance, the iso-response diagram (Fig. 8a) highlights mixes DSC2, DSC3, and DSC4 as high-performing mixes, achieving 7-day compressive strengths of 19–21 MPa, as listed in Table 4.

These results indicate that the short-term strength increase is primarily due to the physical effects of the fillers rather than the pozzolanic activity of WGP. Notably, the pozzolanic reaction between WGP and calcium hydroxide released during cement hydration occurs at a slower rate, contributing to higher strength indices at later ages (beyond 56 days) rather than at earlier ages (7 days) [62, 63]. In their study, Afshinnia and Rangaraju [64] demonstrated that fine WGP can act as an efficient pozzolanic element when used as a cement replacement up to 20% by mass, particularly after 28 days. However, at early ages, the pozzolanic reactivity of WGP remains limited.

This phenomenon also explains the observed reduction in strength when LF is replaced with higher amounts of WGP (80% and 100%) or WEP at all proportions, As shown in Fig. 8a and Table 4, these mixes resulting in 7-day compressive strengths of 11–13 MPa. These findings align with prior studies [65–67].

At 90 days (Fig. 9), the total replacement of LF with 100% WGP (DSC6) yielded a significant increase in compressive strength, reaching 56.77%, with a strength value of 41.89 MPa. Conversely, the total replacement of LF with WEP (DSC11) resulted in a reduction in compressive strength, with a total replacement yielding 22.45 MPa (a 16% decrease). The notable strength increase between 7 and 90 days can be attributed to the pozzolanic activity of

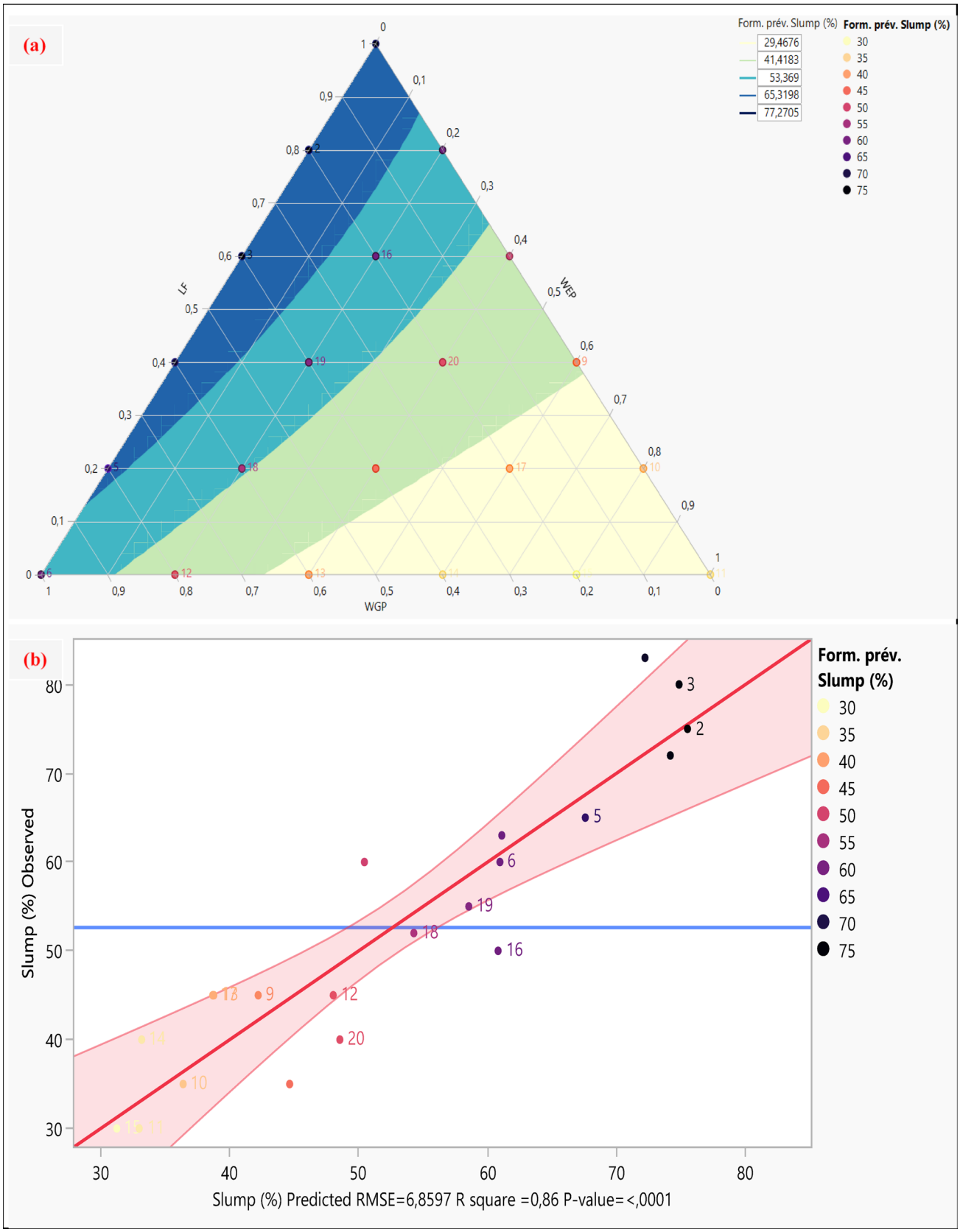

Fig. 7 **a** Iso-response curves illustrating spread results obtained using the shock table **b** Correlation curve comparing observed values with predicted values for spread

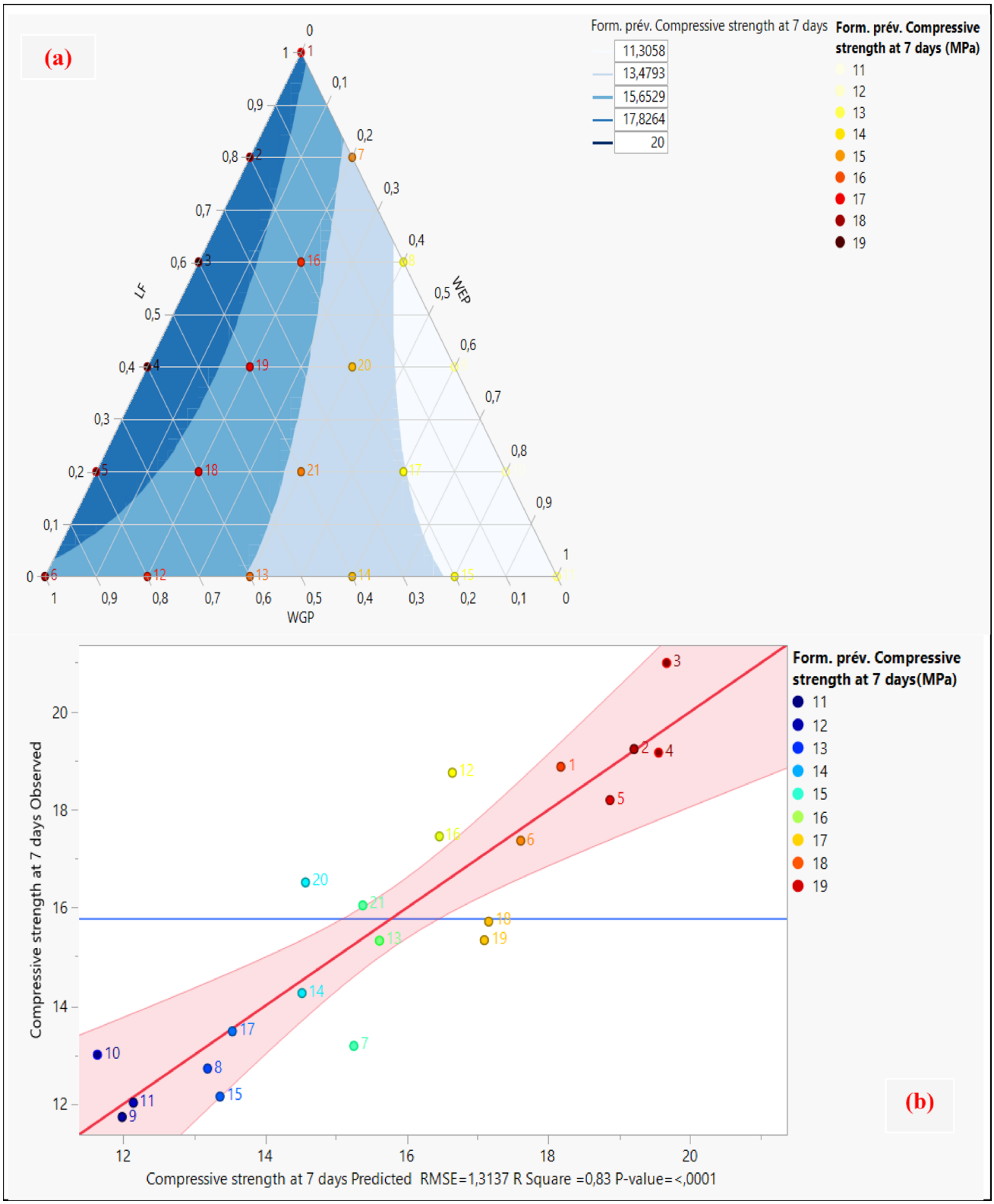

Fig. 8 **a** Iso-response curves illustrating 7-day compressive strength **b** Correlation curve comparing experimental (observed) and predicted results

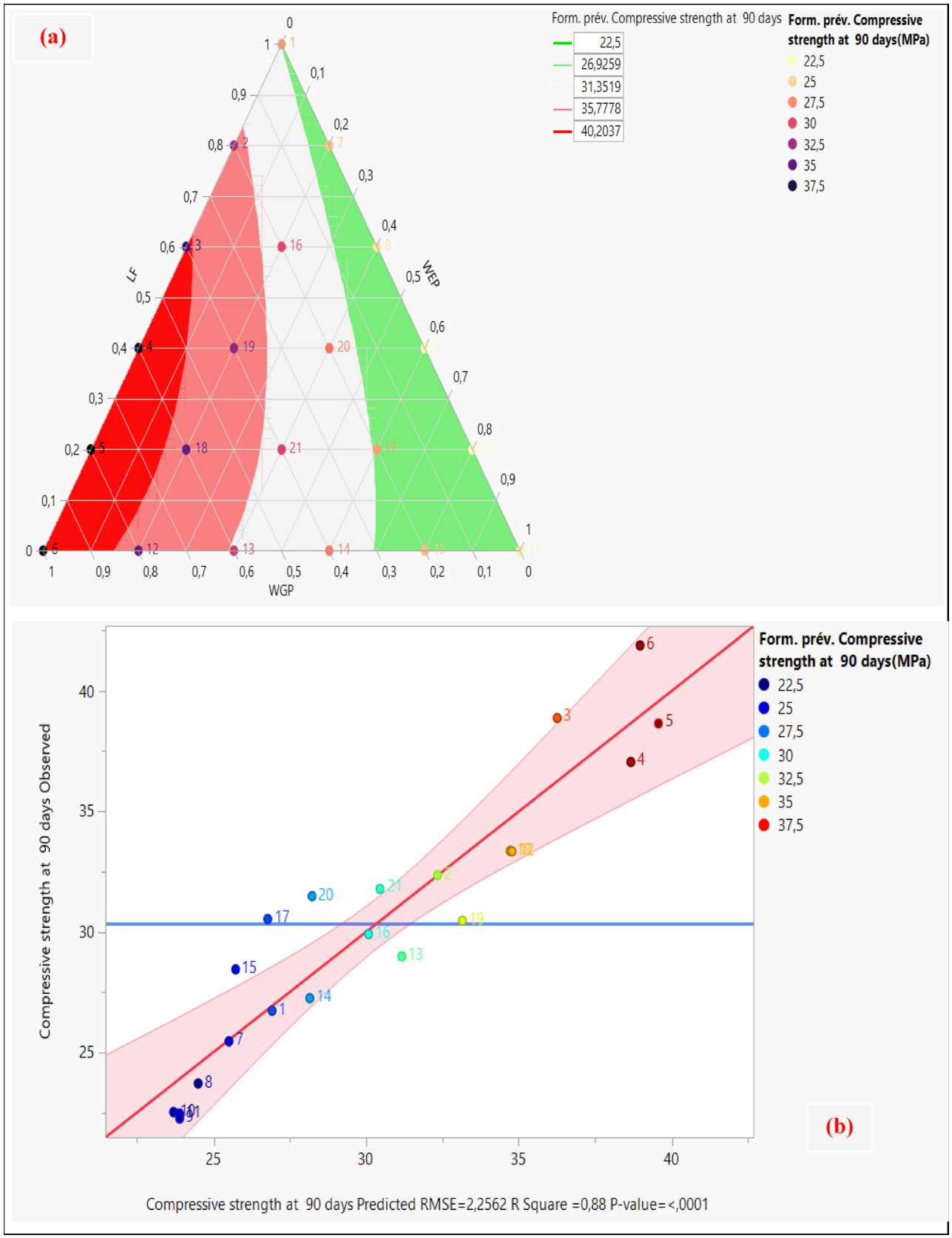

Fig. 9 **a** Iso-response curves illustrating 90-day compressive strength **b** Correlation curve comparing experimental (observed) and predicted results

both glass and perlite, as reported by other researchers [64, 68, 69].

The reduction in strength with WEP additions (Fig. 10) can be explained by variations in particle size, surface texture, particle size distribution, and the slower pozzolanic reactivity of perlite, consistent with other studies [44, 70].

In general, higher proportions of WGP and LF result in greater compressive strength, with WGP having a more pronounced effect. This is evident in the iso-response diagram (Fig. 9), and corroborated by the values in Table 4. In contrast, increasing the proportion of WEP in the mixes leads to a decrease in compressive strength. However, the values obtained remain acceptable compared to those obtained in earlier studies. Notably, ternary mixes combining LF, WGP, and WEP (e, g., at 20%, 40%, and 60% ratios) outperformed the control mix, achieving higher average compressive strengths than the 100% LF refrence.

Thermal conductivity

Figure 11 presents the thermal conductivity values of the studied sand concretes, highlighting the effects of incorporating recycled WGP and WEP, either as total or partial replacements or combined with LF.

To clarify the comparative trends, the mixes containing 100% of each filler material (DSC1, DSC6, and DSC11) are first analyzed. The reference mixture (DSC1), composed solely of LF, exhibits a thermal conductivity value of 1.713 W $m^{-1}.K^{-1}$. In contrast, the mixture containing only WGP (DSC6) achieves a lower thermal conductivity value of 1.568 W $m^{-1}.K^{-1}$, while the mixture composed only WEP (DSC11) demonstrates the lowest thermal conductivity value of 1.451 W $m^{-1}.K^{-1}$. These values, as also reported in Table 4**,** indicate that replacing LF with either WEP or WGP significantly reduced the thermal conductivity of the concrete, with WEP exhibiting the most favorable effect.

The iso-response curves in Fig. 11 further confirm that the full replacement of LF with WGP or WEP results in reductions in thermal conductivity by 8.46% and 15.29%, respectively. The trend observed across mixtures in Table 4 and Fig. 11 shows that inceasing the WEP proportion consistently decreases thermal conductivity. These observations align with findings from previous studies, which suggest that thermal conductivity is influenced not only by porosity but also by the mineralogical composition of these materials [71].

As shown in Table 4, adding WEP reduces the density of DSC, which plays a dual role: first, by lowering the bulk mass, and second, through its porous microstructure and intrinsic-low thermal conductivity (approximately 0.04 W $m^{-1}.K^{-1}$), which contribute to imroved thermal insulation [59, 60].

For comparison, Zhang et al. [44] investigated the effect of expanded perlite (EP) content ground to sizes smaller than 44 µm on the thermal insulation performance of lightweight aggregate geopolymer concrete. They found that replacing metakaolin and ground granulated blast furnace slag with 50% expanded perlite yielded a lightweight, thermally insulating, eco-friendly construction material, supporting the potential of WEP as a sustainable thermal modifier.

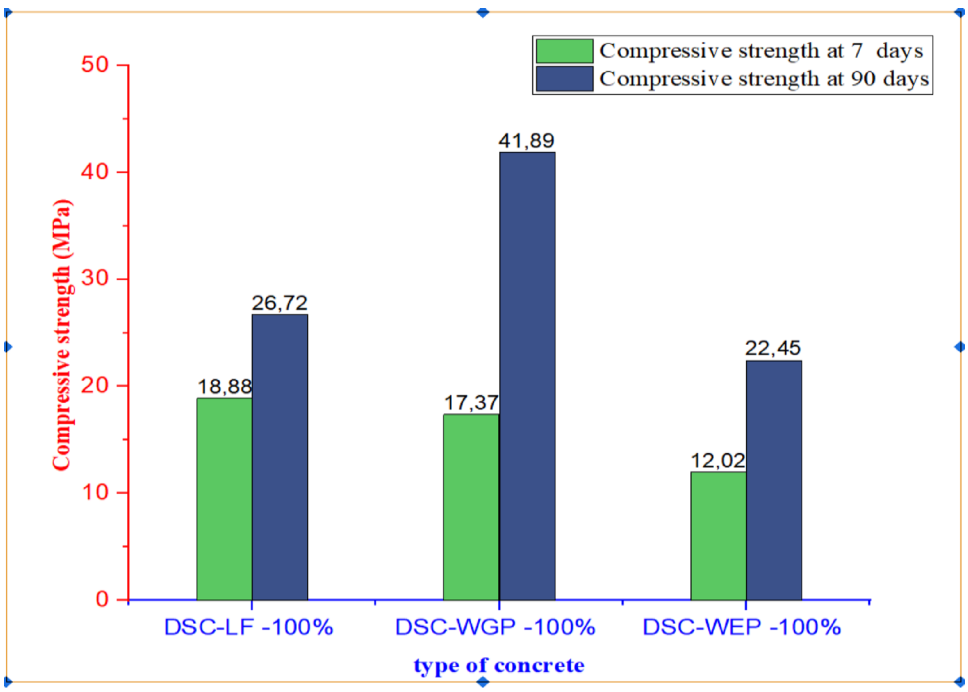

Fig. 10 Compressive strength at 7 and 90 days for mixtures composed of 100% of each type (LF- WGP–WEP)

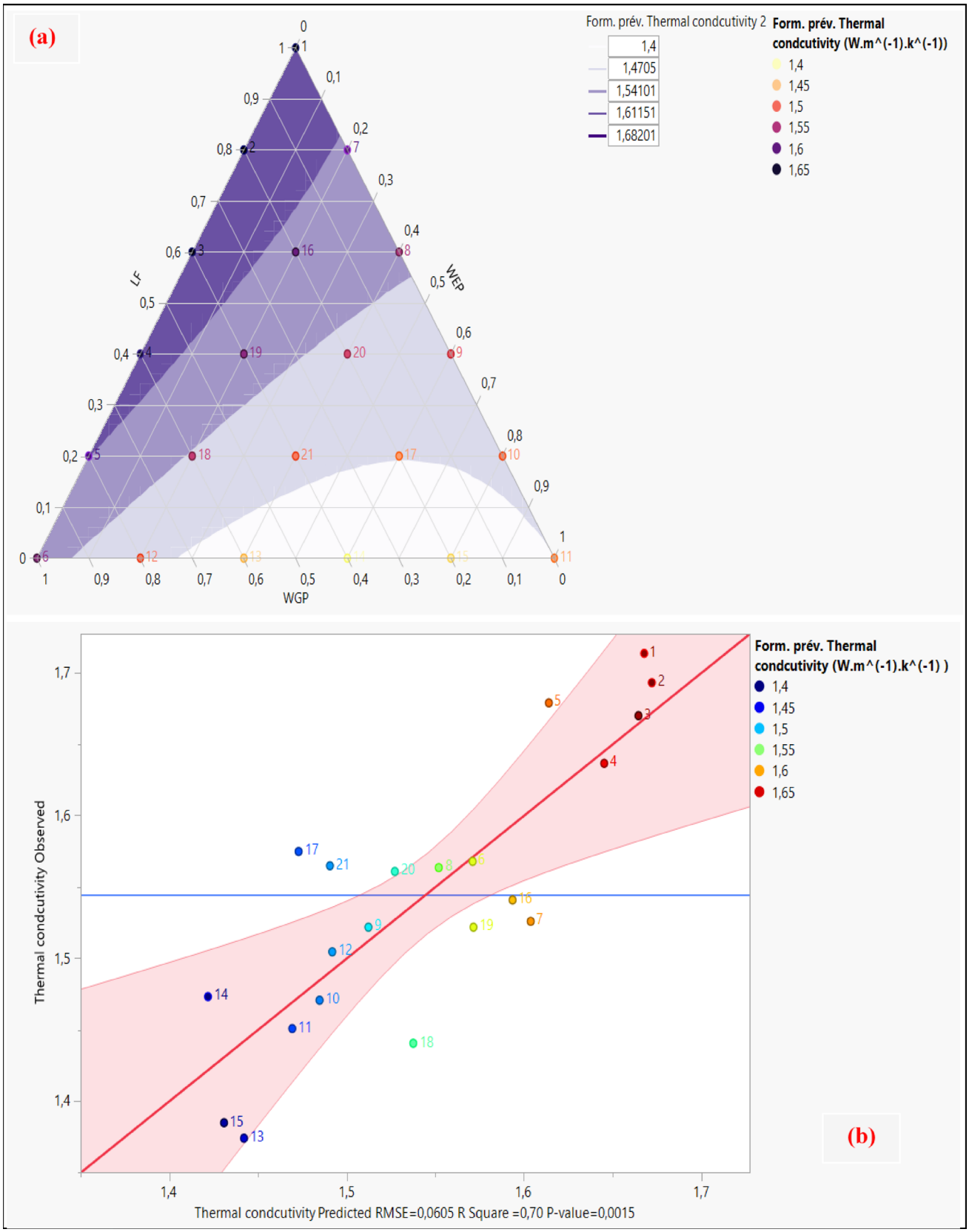

Fig.11 **a** Iso-response curves for thermal conductivity **b** Correlation curve comparing experimental (observed) and theoretical (predicted) results for thermal conductivity

Water absorption

Sand concrete generally exhibits a higher water absorption capacity than ordinary concrete due to its sand-based granular composition [72]. Water absorption is widely regarded as a critical parameter for evaluating the durability of cementitious composites. According to J. Castro et al. [73], concrete quality can be categorized based on its water absorption percentage:

- High-quality concrete: absorption percentage below 3%,
- Medium-quality concrete: absorption percentage between 3 and 5%,
- Poor-quality concrete: absorption percentage exceeding 5%.

As shown in the iso-response curves Fig. 12, and supported by numerical values inTable 4, increasing WGP content in the mix leads to a significant reduction in water absorption. For instance, the full replacement of LF with WGP (mix DSC6) results in a 35.52% reduction. This reduction is attributed to WGP's ability to decrease total porosity and reduce the size of the most probable pores, leading to a denser microstructure. These improvements arise from WGP's pozzolanic properties and its role in filling voids within the cement matrix.

These findings align with previous research, which has shown that pozzolanic materials such as WGP produce reaction products that fill capillary pores, reducing the permeability of concrete and consequently improving the durability [74, 75]. For instance, the study of Patel et al. [74] reported that replacing 20% of cement with WGP reduced water absorption by 30%.

On the other hand, when LF is fully replaced by WEP, the absorption values remain approximately similar to those of the reference concrete. This suggests that WEP does not provide the same pore-filling or densifying effects as WGP.

Microstructural analysis

Figures 13, 14, 15, and 16 present SEM images of mixes DSC1, DSC6, corresponding to compositions of 100% LF, 100% WGP, and 100% WEP, respectively. The analysis also includes mix DSC19, which contains a ternary combination of 40% LF, 40% WGP, and 20% WEP to provide a broader understanding. This particular mixture demonstrated slightly higher mechanical strength and lower thermal conductivity compared to the reference concrete (100% LF).

The SEM images reveal the presence of C–S–H gel along with hexagonal plates of $Ca(OH)_2$ crystals. The inclusion of $Ca(OH)_2$ within the C–S–H gel appears to be a key factor contributing to improved mechanical strength [75]. However, mix DSC11 (100% WEP) exhibits a less homogeneous microstructure with visible micropores, indicating poor particle compaction. This observation is consistent with the reduced mechanical strength compared to the control concrete, as presented in Table 4.

Mixes DSC6 (100% WGP), DSC1 (100% LF), and DSC19 (40% LF + 40% WGP + 20% WEP) display more uniform and compact microstructures. These mixes contain a greater amount of C-S–H gel and $Ca(OH)_2$ crystals, highlighting the combined effects of LF's filling properties and WGP's superior pozzolanic activity.

The EDX analysis of mix DSC6 (100% WGP), as shown in Fig. 14, reveals high-intensity peaks for calcium and silica, with significantly broader silica peaks compared to mixes DSC1, DSC11, and DSC19. The dissolved silica reacts with hydrated lime ($Ca(OH)_2$) to form additional C-S–H phases, contributing to a denser microstructure and higher compressive strength [12, 76].

The FE-SEM and EDX results further confirm that the ternary combination of LF, WGP, and WEP enhances the microstructural properties of the material. This mix achieves a more homogeneous and denser structure with improved strength, effectively addressing the filling deficiencies observed in the DSC11 mix (100% WEP).

Conclusions

This study investigated the incorporation of LF, WGP, and WEP into DSC. The main findings are summerized as follows:

- Combining LF and WGP in different proportions improved workability, DSC2, DSC3, and DSC4, where LF and WGP varied from 20 to 80%, with enhancements of approximately 4.16%, 11.11%, and 15.27%, respectively. However, higher WGP proportions (80% and 100%) reduced the workability, though still within ASTM C1437 standards. Adding WEP generally decreased workability.
- Replacing LF with WGP or WEP progressively decreased the thermal conductivity. At full replacement, reductions of 8.46% and 15.29%, while ternary use of LF, WGP, and WEP showed reductions ranged from 8.67 to 15.92%.
- WGP significantly enhanced long-term strength, reaching 41 MPa at 90 days (56% increase). Although WEP slightly reduced strength, all ternary mixtures surpassed the control concrete, with improvements ranging from 11.9 to 24.85%.
- Full replacement of LF with WGP decreased water absorption by ~ 35.5%. Ternary blends reduced absorption

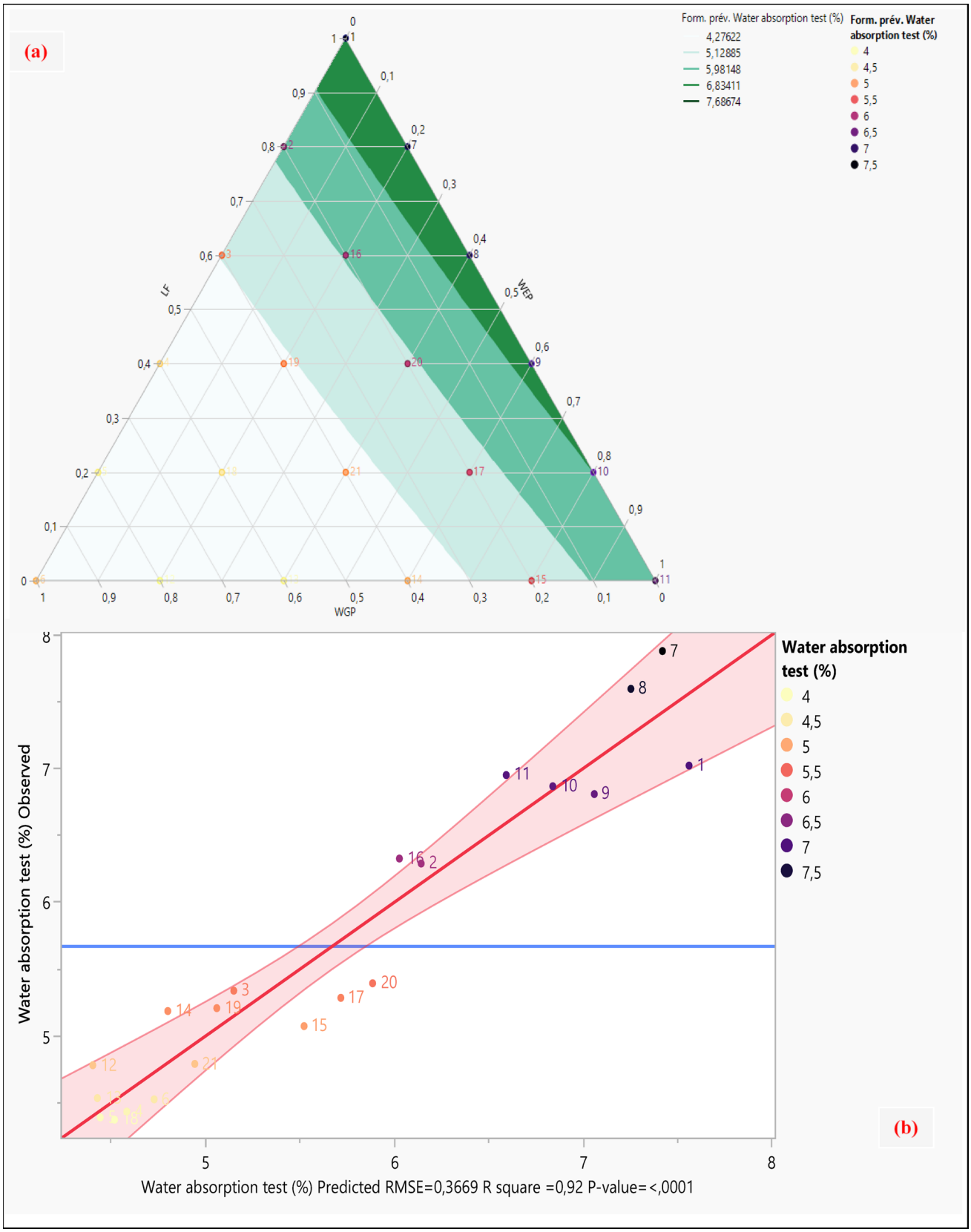

Fig. 12 **a** Iso-response curve for water absorption **b** Correlation curve comparing experimental (observed) and theoretical (predicted) results for water absorption

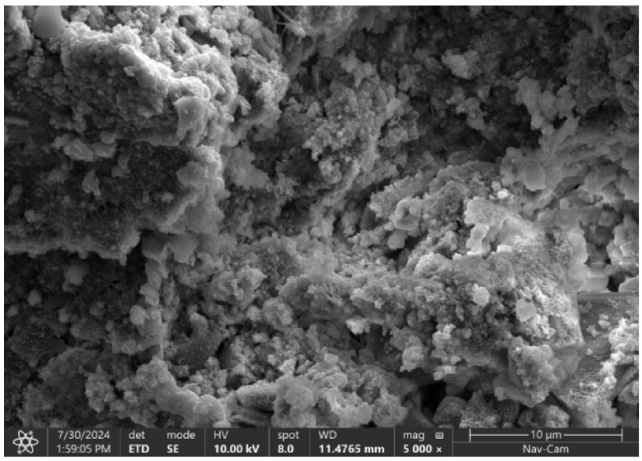

SEM image - G=5000

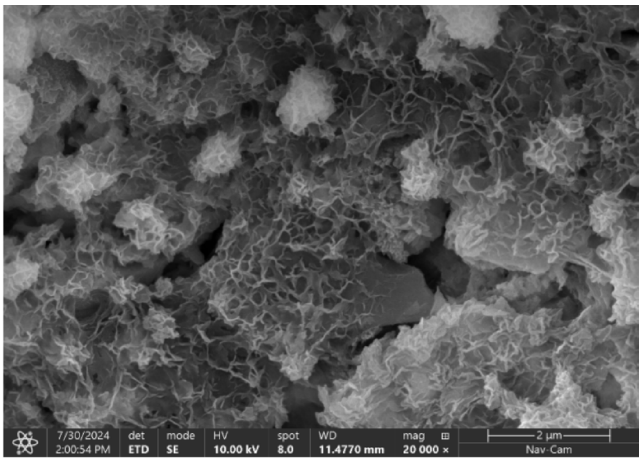

SEM image - G=20000

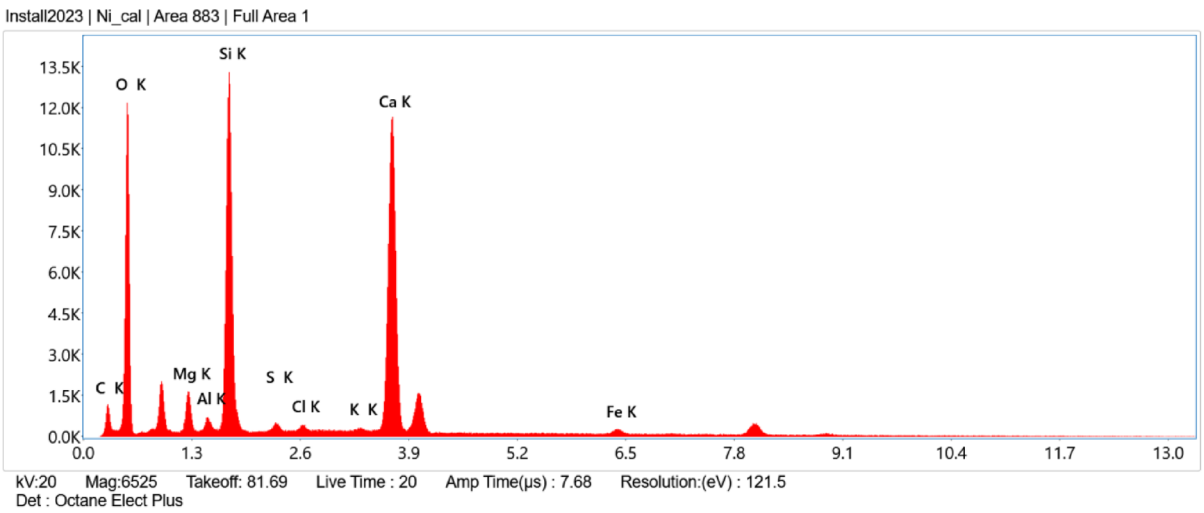

EDX spectrum indicating elemental composition

Fig. 13 FE-SEM/EDX analyses of DSC1 composition (100% LF)

by 10–38%, while WEP-only mixes remained comparable to the control.

- SEM revealed compact, uniform microstructures in LF–WGP mixtures, rich in C–S–H and $Ca(OH)_2$. WEP-based mixes showed increased microporosity, explaining slight reductions in strength.
- EDX confirmed that higher WGP content led to increased Ca and Si peaks, indicating active pozzolanic reactions and reduced pore volume.

Notably, using WGP and WEP in DSC promotes waste valorization, reduces environmental impacts, and supports circular economy goals, particularly in arid regions. To further validate the practical performance of these mixtures, future research should focus on durability aspects such as sulfate resistance, freeze–thaw behavior, carbonation, and chloride ion penetration. Field-scale validation is also recommended. Moreover, advanced microstructural investigations (e.g., XRD, FTIR, and TGA) are encouraged to deepen the understanding of the pozzolanic mechanisms involved.

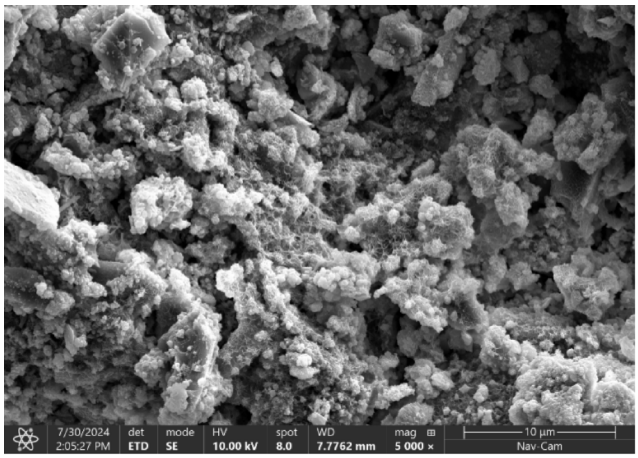

SEM image - G=5000

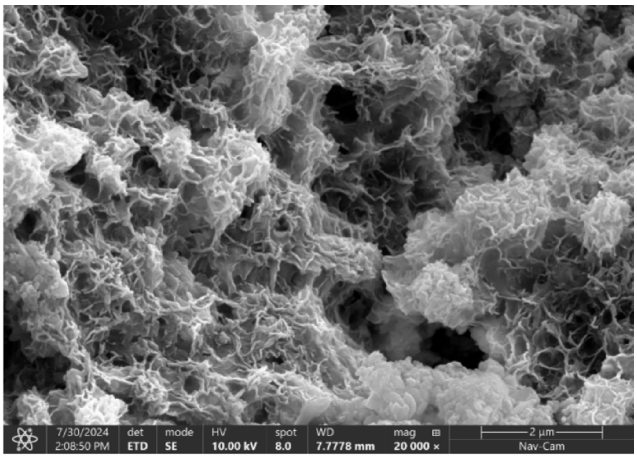

SEM image - G=20000

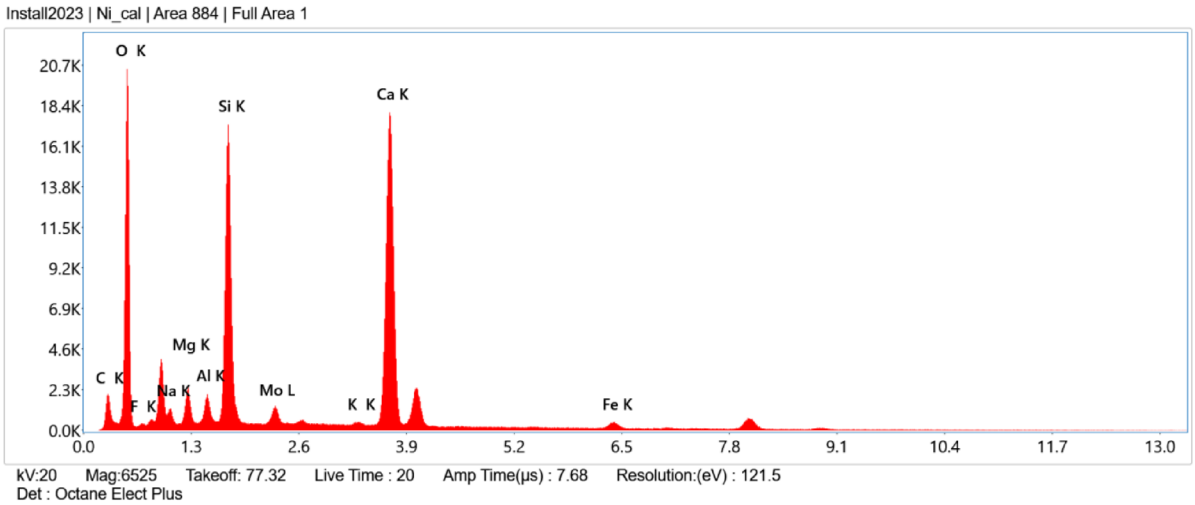

EDX spectrum indicating elemental composition

Fig. 14 FE-SEM/EDX analyses of DSC 6 (100% WGP)

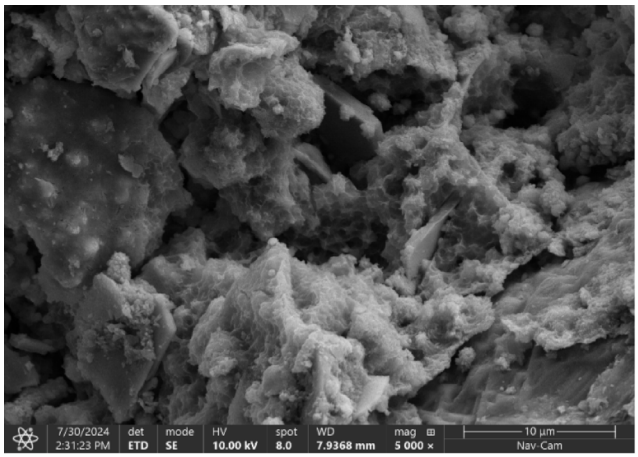

SEM image - G=5000

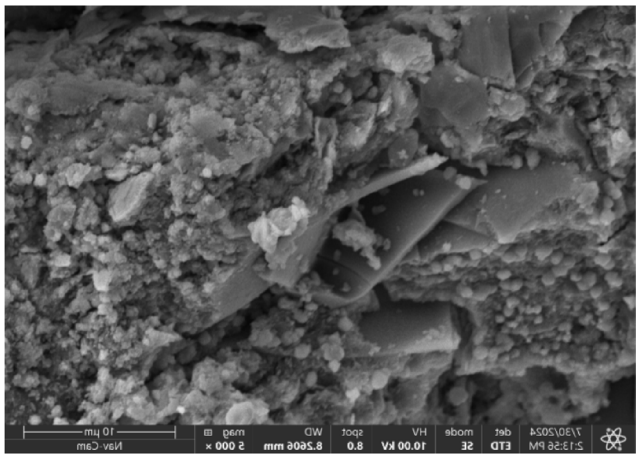

SEM image - G=5000

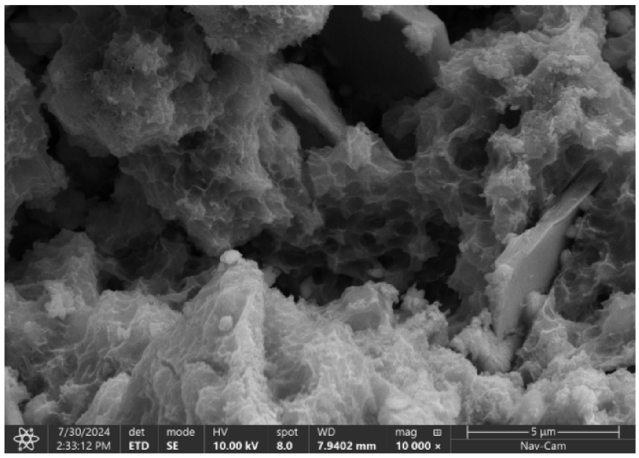

SEM image - G=10000

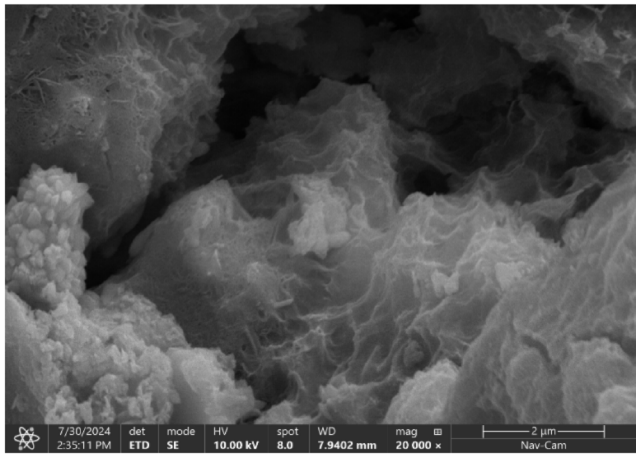

SEM image - G=20000

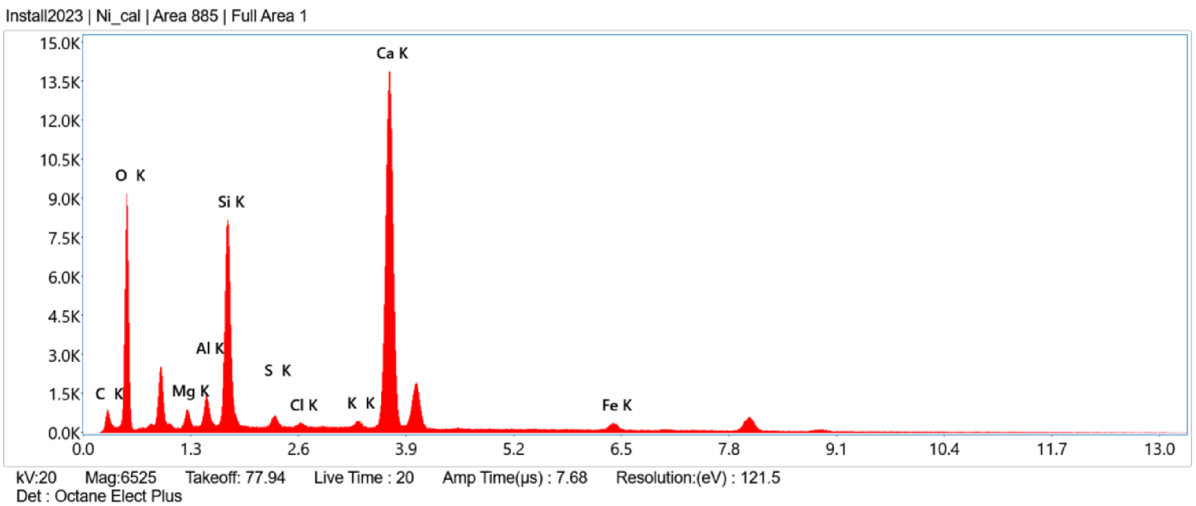

EDX spectrum indicating elemental composition

Fig. 15 FE-SEM/EDX analyses of DSC11 (100% WEP)

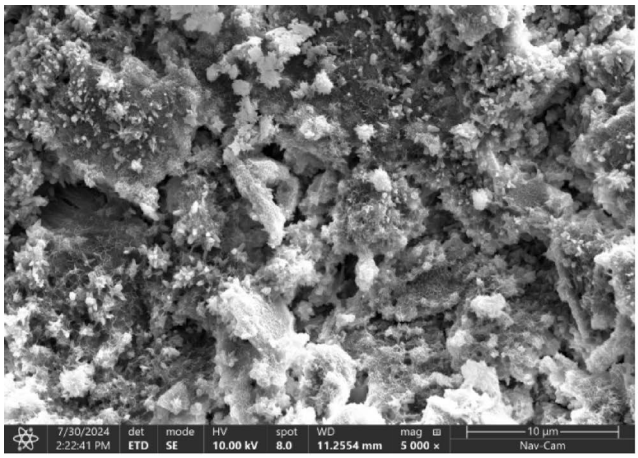

SEM image - G=5000

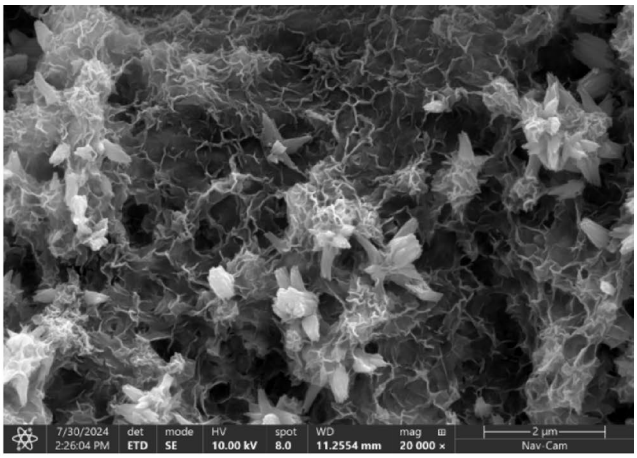

SEM image - G=20000

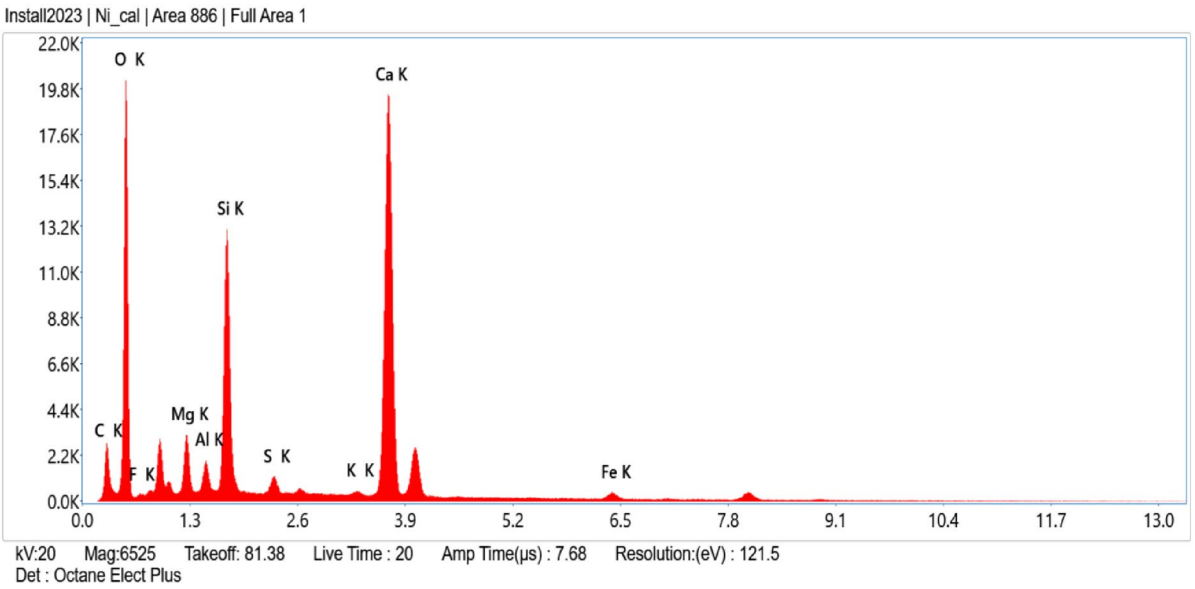

EDX spectrum indicating elemental composition

Fig. 16 FE-SEM/EDX analyses of DSC19 (40% LF + 40% WGP + 20% WEP)

Acknowledgements The authors would like to thank the General Directorate of Scientific Research and Technological Development of Algeria (DGRSDT) for its support.

Author contributions MM contributed to resources, visualization and draft paper writing; MB and AM contributed to conceptualization, methodology, writing—review and editing and supervision; LP contributed to writing—review and editing, AN contributed to resources.

Funding Not applicable.

Data availability The data of this study are available on request from the corresponding author.

Code availability Not applicable.

Declarations

Conflict of interest The authors declare no conflicts of interests related to this research.

Human or animal rights This study does not involve human participant or animals.

Informed consent Not applicable.

References

1. Vo T, Wiliam N, Del MG et al (2022) Coal mining wastes valorization as raw geomaterials in construction: a review with new perspectives. J Clean Prod 336:130213. https://doi.org/10.1016/j.jclepro.2021.130213
2. Beddar M, Meddah A, Belagraa L (2017) Feasibility of using fibrous waste in cement-based material. IOP Conf Ser Mater Sci Eng 246:012034. https://doi.org/10.1088/1757-899X/246/1/012034
3. Meddah A, Beddar M, Bali A (2014) Use of shredded rubber tire aggregates for roller compacted concrete pavement. J Clean Prod 72:187–192. https://doi.org/10.1016/j.jclepro.2014.02.052
4. Meddah A, Chikouche MA, Yahia M et al (2022) The efficiency of recycling expired cement waste in cement manufacturing: a sustainable construction material. Circ Econ Sustain 2:1213–1224. https://doi.org/10.1007/s43615-022-00161-1
5. Wang M, Zhao L, Niu Z, Sadeghzadeh SM (2024) Mitigating CO2 emanations within the marine concrete industry with different structures of silica nanoparticles. Case Stud Constr Mater 20:e03033. https://doi.org/10.1016/j.cscm.2024.e03033
6. Zhao L, Wang M, Zhang L, Sadeghzadeh SM (2024) Impact of chitosan extracted from shrimp shells on the shrinkage and mechanical properties of cement-based composites using dendritic fibrous nanosilica. Heliyon 10:e31576. https://doi.org/10.1016/j.heliyon.2024.e31576
7. Al-Oraimi S, Taha R, Hassan H (2006) The effect of the mineralogy of coarse aggregate on the mechanical properties of high-strength concrete. Constr Build Mater 20:499–503. https://doi.org/10.1016/j.conbuildmat.2004.12.005
8. Hasdemir S, Tuğrul A, Yılmaz M (2016) The effect of natural sand composition on concrete strength. Constr Build Mater 112:940–948. https://doi.org/10.1016/j.conbuildmat.2016.02.188
9. Huynh T-P, Ho LS, Ho QV (2022) Experimental investigation on the performance of concrete incorporating fine dune sand and ground granulated blast-furnace slag. Constr Build Mater 347:128512. https://doi.org/10.1016/j.conbuildmat.2022.128512
10. Krishna RS, Elshorbagi M, Tao Z et al (2025) Enhancing desert sand concrete with fibre-reinforced polymer (FRP) confinement: mechanical and microstructural perspectives. Sustain Mater Technol 45:e01503. https://doi.org/10.1016/j.susmat.2025.e01503
11. Hamada HM, Abed F, Katman HYB et al (2023) Effect of silica fume on the properties of sustainable cement concrete. J Mater Res Technol. https://doi.org/10.1016/j.jmrt.2023.05.147
12. Zhang M, Zhu X, Shi J et al (2022) Utilization of desert sand in the production of sustainable cement-based materials: a critical review. Constr Build Mater 327:127014. https://doi.org/10.1016/j.conbuildmat.2022.127014
13. Bédérina M, Khenfer MM, Dheilly RM, Quéneudec M (2005) Reuse of local sand: effect of limestone filler proportion on the rheological and mechanical properties of different sand concretes. Cem Concr Res 35:1172–1179. https://doi.org/10.1016/j.cemconres.2004.07.006
14. Yang H, Jiao Y, Xing J, Liu Z (2024) Statistical model and fracture behavior of manufactured sand concrete with varying replacement rates and stone powder contents. J Build Eng 95:110102
15. Kaufmann J (2020) Evaluation of the combination of desert sand and calcium sulfoaluminate cement for the production of concrete. Constr Build Mater 243:118281
16. Wang L, Xiao W, Wang Q et al (2022) Freeze-thaw resistance of 3D-printed composites with desert sand. Cem Concr Compos 133:104693. https://doi.org/10.1016/j.cemconcomp.2022.104693
17. Dong W, Shen X, Xue H et al (2016) Research on the freeze-thaw cyclic test and damage model of aeolian sand lightweight aggregate concrete. Constr Build Mater 123:792–799
18. Paul D, Bindhu KR, Matos AM, Delgado J (2022) Eco-friendly concrete with waste glass powder: a sustainable and circular solution. Constr Build Mater 355:129217
19. Yehia SA, Shahin RI, Fayed S (2024) Compressive behavior of eco-friendly concrete containing glass waste and recycled concrete aggregate using experimental investigation and machine learning techniques. Constr Build Mater 436:137002. https://doi.org/10.1016/J.CONBUILDMAT.2024.137002
20. Ahmed SN, Sor NH, Ahmed MA, Qaidi SMA (2022) Thermal conductivity and hardened behavior of eco-friendly concrete incorporating waste polypropylene as fine aggregate. Mater Today Proc 57:818–823. https://doi.org/10.1016/J.MATPR.2022.02.417
21. Omran A, Tagnit-Hamou A (2016) Performance of glass-powder concrete in field applications. Constr Build Mater 109:84–95. https://doi.org/10.1016/J.CONBUILDMAT.2016.02.006
22. Islam GMS, Rahman MH, Kazi N (2017) Waste glass powder as partial replacement of cement for sustainable concrete practice. Int J Sustain Built Environ 6:37–44. https://doi.org/10.1016/J.IJSBE.2016.10.005
23. Du Y, Yang W, Ge Y et al (2021) Thermal conductivity of cement paste containing waste glass powder, metakaolin and limestone filler as supplementary cementitious material. J Clean Prod 287:125018. https://doi.org/10.1016/J.JCLEPRO.2020.125018
24. Afshinnia K, Rangaraju PR (2016) Impact of combined use of ground glass powder and crushed glass aggregate on selected properties of Portland cement concrete. Constr Build Mater 117:263–272
25. Idir R, Cyr M, Tagnit-Hamou A (2011) Pozzolanic properties of fine and coarse color-mixed glass cullet. Cem Concr Compos 33:19–29. https://doi.org/10.1016/j.cemconcomp.2010.09.013
26. Sikora P, Horszczaruk E, Skoczylas K, Rucinska T (2017) Thermal properties of cement mortars containing waste glass aggregate and nanosilica. Procedia Eng 196:159–166. https://doi.org/10.1016/j.proeng.2017.07.186
27. Maglad AM, Othuman Mydin MA, Majeed SS et al (2023) Development of eco-friendly foamed concrete with waste glass sheet powder for mechanical, thermal, and durability properties enhancement. J Build Eng 80:107974
28. Ammari MS, Tobchi MB, Amrani Y et al (2023) Influence of glass powder incorporation on the physical-mechanical properties of sand concrete. World J Eng 20:314–324. https://doi.org/10.1108/WJE-08-2021-0474
29. Shayan A, Xu A (2006) Performance of glass powder as a pozzolanic material in concrete: a field trial on concrete slabs. Cem Concr Res 36:457–468. https://doi.org/10.1016/j.cemconres.2005.12.012
30. Rashad AM (2016) A synopsis about perlite as building material – a best practice guide for civil engineer. Constr Build Mater 121:338–353
31. Long W-J, Tan X-W, Xiao B-X et al (2019) Effective use of ground waste expanded perlite as green supplementary cementitious material in eco-friendly alkali activated slag composites. J Clean Prod 213:406–414. https://doi.org/10.1016/j.jclepro.2018.12.118
32. Kotwica Ł, Pichór W, Nocuń-Wczelik W (2016) Study of pozzolanic action of ground waste expanded perlite by means of thermal methods. J Therm Anal Calorim 123:607–613. https://doi.org/10.1007/s10973-015-4910-8
33. Kotwica Ł, Pichór W, Kapeluszna E, Różycka A (2017) Utilization of waste expanded perlite as new effective supplementary cementitious material. J Clean Prod 140:1344–1352. https://doi.org/10.1016/j.jclepro.2016.10.018

34. Pichór W, Barna M, Kapeluszna E et al (2015) The influence of waste expanded perlite on chemical durability of mortars. Solid State Phenom 227:194–198. https://doi.org/10.4028/WWW.SCIENTIFIC.NET/SSP.227.194
35. ENPC (1994) SABLOCRETE. Projet National de Recherche/Développement. (1994). Bétons de sable: caractéristiques et pratiques d'utilisation
36. Hadjoudja M, Benzaid R, Mesbah H-A et al (2021) Effect of mineral additions and metal fibers on the resistance of cracking of the dune sand concretes. Iran J Sci Technol Trans Civ Eng 45:1523–1537. https://doi.org/10.1007/s40996-021-00647-2
37. Boucedra A, Bederina M, Ghernouti Y (2020) Study of the acoustical and thermo-mechanical properties of dune and river sand concretes containing recycled plastic aggregates. Constr Build Mater 256:119447. https://doi.org/10.1016/j.conbuildmat.2020.119447
38. Bouziani T, Bederina M, Hadjoudja M (2012) Effect of dune sand on the properties of flowing sand-concrete (FSC). Int J Concr Struct Mater 6:59–64. https://doi.org/10.1007/s40069-012-0006-z
39. Belhadj B, Bederina M, Makhloufi Z et al (2015) Study of the thermal performances of an exterior wall of barley straw sand concrete in an arid environment. Energy Build 87:166–175. https://doi.org/10.1016/j.enbuild.2014.11.034
40. Ammari MS, Bederina M, Belhadj B et al (2021) Effect of barley straw treatments on desiccation shrinkage and thermal properties of lightweight sand concrete ARTICLE INFO ABSTRACT/RESUME. Alger J Environ Sci 7:2037–2044
41. EN-197-1 (2001) Standard: cement: composition, specifications and conformity criteria for common cements. Part 1
42. Awolusi TF, Oke OL, Akinkurolere OO, Sojobi AO (2019) Application of response surface methodology: predicting and optimizing the properties of concrete containing steel fibre extracted from waste tires with limestone powder as filler. Case Stud Constr Mater 10:e00212. https://doi.org/10.1016/j.cscm.2018.e00212
43. Bao S, Zhang Y, Liu H et al (2023) Flexural behavior of the UHPCC containing glass powder as partial substitute of cement/silica fume. Constr Build Mater 365:130142
44. Zhang YH, Wang H, Zhong WL, Fan LF (2024) Development of a high-strength lightweight geopolymer concrete for structural and thermal insulation applications. Case Stud Constr Mater 21:e03949. https://doi.org/10.1016/J.CSCM.2024.E03949
45. -2 E (2012) EN 934-2:2009+A1:2012 – Admixtures for concrete, mortar and grout – Part 2: Concrete admixtures – Definitions, requirements, conformity, marking and labelling. European Committee for Standardization
46. Hamla W, Benamara D, Noui A (2022) Statistical modeling of physical and mechanical responses of roller-compacted sand concrete made with ternary sand using the experimental design method. Constr Build Mater 345:128354
47. Benkhelil M, Arroudj K, Guettala S, Douara T-H (2023) Prediction of the physico-mechanical characteristics of a high-performance concrete containing dune sand powder and ground blast-furnace slag. Constr Build Mater 398:132482
48. Goupy JCL (2007) Introduction to design of experiments with JMP examples. SAS Publishing, Hojai
49. Tahar Z, Assia A, Mouloud B et al (2023) Combined sand eco-mortar reinforced with polyethylene Terephthalate: behavior and optimization using RSM method. Constr Build Mater 404:133160. https://doi.org/10.1016/j.conbuildmat.2023.133160
50. Jacques G, Lee C (2007) Introduction to design of experiments with JMP examples. SAS Publishing, Hojai
51. ASTM (2000) Standard test method for flow of hydraulic cement mortar. ASTM, Pennsylvania
52. ASTM (2021) Standard test method for density, absorption, and voids in hardened concrete. ASTM, Pennsylvania
53. AFNOR (2019) Essais pour béton durci - Partie 5: résistance à la flexion des éprouvettes NF EN 12390-5
54. Afnor (2019) Essais pour béton durci - Partie 4: résistance à la compression - Caractéristiques des machines d'essai. NF EN 12390-4
55. Zaitri R, Bederina M, Bouziani T et al (2014) Development of high performances concrete based on the addition of grinded dune sand and limestone rock using the mixture design modelling approach. Constr Build Mater 60:8–16. https://doi.org/10.1016/j.conbuildmat.2014.02.062
56. Abderraouf Belkadi A, Kessal O, Berkouche A et al (2024) Experimental investigation into the potential of recycled concrete and waste glass powders for improving the sustainability and performance of cement mortars properties. Sustain Energy Technol Assess 64:103710. https://doi.org/10.1016/j.seta.2024.103710
57. Rahma A, El Naber N, Issa Ismail S (2017) Effect of glass powder on the compression strength and the workability of concrete. Cogent Eng. https://doi.org/10.1080/23311916.2017.1373415
58. Różycka A, Pichór W (2016) Effect of perlite waste addition on the properties of autoclaved aerated concrete. Constr Build Mater 120:65–71
59. Sengul O, Azizi S, Karaosmanoglu F, Tasdemir MA (2011) Effect of expanded perlite on the mechanical properties and thermal conductivity of lightweight concrete. Energy Build 43:671–676. https://doi.org/10.1016/j.enbuild.2010.11.008
60. Liu WV, Apel DB, Bindiganavile VS (2014) Thermal properties of lightweight dry-mix shotcrete containing expanded perlite aggregate. Cem Concr Compos 53:44–51. https://doi.org/10.1016/j.cemconcomp.2014.06.003
61. Wild S, Khatib JM, Jones A (1996) Relative strength, pozzolanic activity and cement hydration in superplasticised metakaolin concrete. Cem Concr Res 26:1537–1544. https://doi.org/10.1016/0008-8846(96)00148-2
62. Shi C, Wu Y, Riefler C, Wang H (2005) Characteristics and pozzolanic reactivity of glass powders. Cem Concr Res 35:987–993. https://doi.org/10.1016/j.cemconres.2004.05.015
63. Li A, Qiao H, Li Q et al (2021) Study on the performance of pervious concrete mixed with waste glass powder. Constr Build Mater 300:123997
64. Afshinnia K, Rangaraju P (2015) Influence of fineness of ground recycled glass on mitigation of alkali–silica reaction in mortars. Constr Build Mater 81:257–267. https://doi.org/10.1016/j.conbuildmat.2015.02.041
65. Corinaldesi V, Gnappi G, Moriconi G, Montenero A (2005) Reuse of ground waste glass as aggregate for mortars. Waste Manag 25:197–201
66. Soliman NA, Tagnit-Hamou A (2016) Development of ultra-high-performance concrete using glass powder – towards ecofriendly concrete. Constr Build Mater 125:600–612. https://doi.org/10.1016/j.conbuildmat.2016.08.073
67. Aliabdo AA, Abd Elmoaty AM, Aboshama AY (2016) Utilization of waste glass powder in the production of cement and concrete. Constr Build Mater 124:866–877. https://doi.org/10.1016/j.conbuildmat.2016.08.016
68. Bektas F, Turanli L, Research PM-C (2005) Undefined use of perlite powder to suppress the alkali–silica reaction. Elsevier, Amsterdam
69. Ramezanianpour A, Mahmoud Motahari Karein B, Vosoughi P et al (2014) Effects of calcined perlite powder as a SCM on the strength and permeability of concrete. Constr Build Mater 66:222–228. https://doi.org/10.1016/j.conbuildmat.2014.05.086
70. Ramdani S, Guettala A, Benmalek M, Aguiar J (2019) Physical and mechanical performance of concrete made with waste rubber aggregate, glass powder and silica sand powder. J Build Eng 21:302–311. https://doi.org/10.1016/j.jobe.2018.11.003

71. Narayanan N, Ramamurthy K (2000) Structure and properties of aerated concrete: a review. Cem Concr Compos 22:321–329. https://doi.org/10.1016/S0958-9465(00)00016-0
72. Projet S Presse de l'Ecole Nationale des Ponts et Chaussées. Bét sable, Caractéristiques Prat d'utilisation Ed Assoc Amicale des Ingénieurs Anciens Elèves L'Ecole Natl des Ponts Chaussées
73. Castro J, Bentz D, Weiss J (2011) Effect of sample conditioning on the water absorption of concrete. Cem Concr Compos. https://doi.org/10.1016/j.cemconcomp.2011.05.007
74. Patel D, Tiwari RP, Shrivastava R, Yadav RK (2019) Effective utilization of waste glass powder as the substitution of cement in making paste and mortar. Constr Build Mater 199:406–415. https://doi.org/10.1016/J.CONBUILDMAT.2018.12.017
75. Payá J, Monzó J, Borrachero MV et al (2018) 17 - bagasse ash. In: Siddique R, Cachim P (eds) Waste and supplementary cementitious materials in concrete. Woodhead Publishing, Cambridge, pp 559–598
76. Ameta N, Wayal A, Hiranandani P (2013) Stabilization of dune sand with ceramic tile waste as admixture. Am J Eng Res 2:133–139